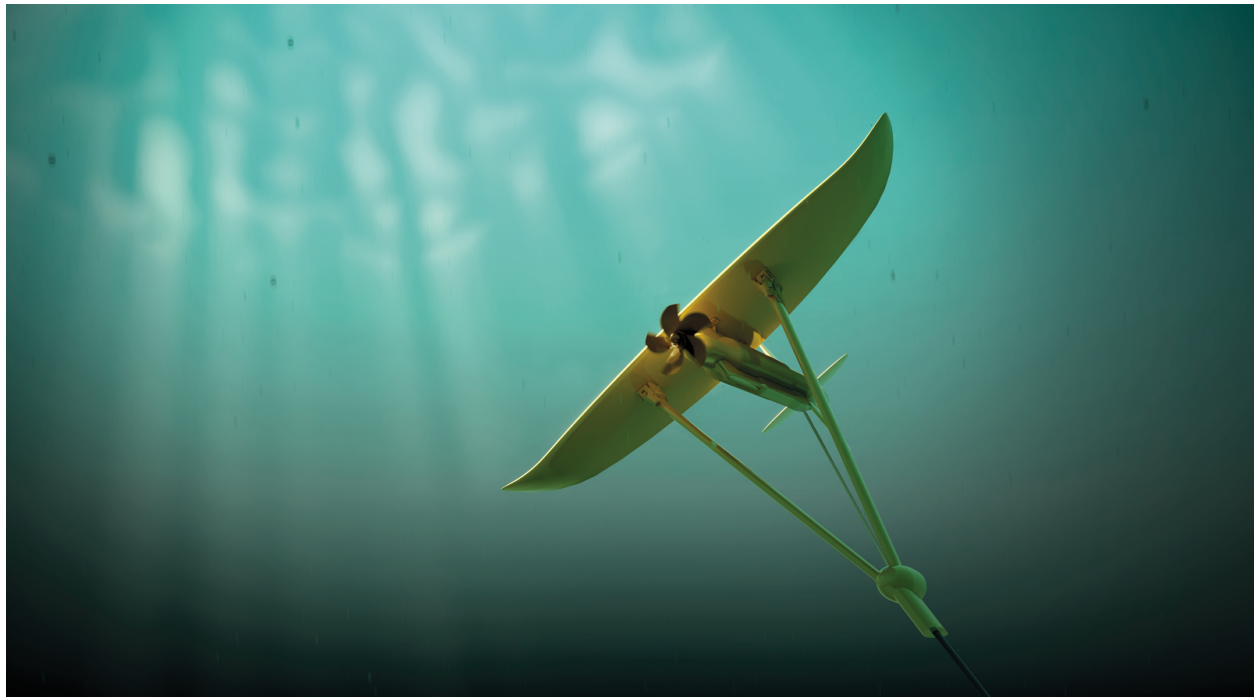




**CHALMERS**  
UNIVERSITY OF TECHNOLOGY

---



# **Overvoltage mitigation of PWM controlled PMSG through long cables for a subsea power plant**

Inverter and filter design for overvoltage reduction

Master's thesis in Master Programme of Electric Power Engineering

Carl Larsson, Andreas Rydgård



MASTER'S THESIS 2018

# **Overvoltage mitigation of PWM controlled PMSG through long cables for a subsea power plant**

Inverter and filter design for overvoltage reduction

CARL LARSSON

ANDREAS RYDGÅRD



**CHALMERS**  
UNIVERSITY OF TECHNOLOGY

Department of Electrical Engineering  
*Division of Electric Power*  
CHALMERS UNIVERSITY OF TECHNOLOGY  
Gothenburg, Sweden 2018

Overvoltage mitigation of PWM controlled PMSG through long cables  
for a subsea power plant  
Inverter and filter design for overvoltage reduction  
CARL LARSSON, ANDREAS RYDGÅRD

Supervisor: Georgios Mademlis, Department of Electrical Engineering  
Magnus Fredriksson, Minesto  
Examiner: Yujing Liu, Department of Electrical Engineering

Master's Thesis 2018  
Department of Electrical Engineering  
Division of Electric Power  
Chalmers University of Technology  
SE-412 96 Gothenburg  
Telephone +46 31 772 1000

Cover: Minestos Deep Green, a concept for a tidal power plant.

Typeset in L<sup>A</sup>T<sub>E</sub>X  
Printed by TeknologTryck  
Gothenburg, Sweden 2018

Overvoltage mitigation of PWM controlled PMSG through long cables  
for a subsea power plant

Inverter and filter design for overvoltage reduction

CARL LARSSON

ANDREAS RYDGÅRD

Department of Electrical Engineering

Chalmers University of Technology

## **Abstract**

With increased need for electric power production that is based on renewable resources it is important to utilize more efficiently the available resources. An emerging technology is a kite moving under-water, which extracts power from the velocity of the ocean currents. By using a wing to create lift from the ocean currents to move through the water, and thereby increase the water flow through the turbine, more power can be produced from the ocean currents. With a power plant moving under water it is preferable to locate as much of the electric components as possible outside of the kite. Locating the inverter away from the power plant creates the need for long transmission lines between the two components. This results in overvoltages at the generator terminal due to reflections of the voltage pulses. This thesis has investigated the problems with overvoltages due to this phenomena and how to mitigate it while keeping only the generator inside the power plant. The study was done through literature study, calculations and simulations in the software LTspice. The results of the thesis show that the overvoltages can be mitigated to an acceptable level below  $\Delta V_{LL} = 20\%$  by implementation of a multilevel converter and an LCR-filter. In addition, by using a 5-level inverter the size of the filter can be reduced while still maintaining an acceptable voltage at the generator terminal.

Keywords: Electric drive, filter, long cable, tidal, power plant, PMSG, kite, generator, subsea, overvoltage mitigation.



## **Acknowledgements**

A great thank you to everyone that has helped us out during the time of this Master's thesis work. A special thank you to Georgios Mademlis for all the help given during this project. It has been a great reassurance to have been able to discuss important parts of the work with you. Thank you Minesto for giving us the opportunity to work with you and get an interesting point of view on our thesis. A special thank you to Magnus Fredriksson for helping out with information and contacts that has made the work more rewarding. Thank you Yujing Liu, our examiner.

Carl Larsson, Andreas Rydgård, Gothenburg, November 2018



# Contents

<b>List of Figures</b>	<b>xiii</b>
<b>List of Tables</b>	<b>xv</b>
<b>1 Introduction</b>	<b>1</b>
1.1 Background . . . . .	1
1.2 Aim . . . . .	3
1.3 Scope . . . . .	3
1.4 Task . . . . .	4
<b>2 Theory</b>	<b>5</b>
2.1 System structure . . . . .	5
2.1.1 System voltages . . . . .	6
2.2 Generator . . . . .	7
2.2.1 PMSG . . . . .	8
2.2.2 Variable speed . . . . .	8
2.2.3 Problems with overvoltage . . . . .	8
2.3 Power electronic converters . . . . .	9
2.3.1 PWM switching . . . . .	9
2.3.2 Topology . . . . .	10
2.3.2.1 2 level PWM . . . . .	10
2.3.2.2 Multilevel PWM . . . . .	11
2.4 Submarine power cable . . . . .	12
2.4.1 Parameters and characteristics of a submarine cable . . . . .	13
2.4.2 Frequency dependency . . . . .	13
2.4.2.1 Skin effect and proximity effect . . . . .	14
2.4.2.2 Hyperbolic correction . . . . .	14
2.4.2.3 Shielding . . . . .	15
2.5 Overvoltage due to wave propagation . . . . .	16
2.5.1 Reflections . . . . .	17
2.5.2 Risetime . . . . .	18
2.5.3 Frequency . . . . .	18
2.5.4 DC magnitude . . . . .	18
2.5.5 Cable length or cable impedance . . . . .	18
2.5.6 System resonance . . . . .	19
2.6 Filter . . . . .	19
2.6.1 Filter design . . . . .	20

2.6.2	Generator side filter . . . . .	21
2.6.2.1	RC filter . . . . .	21
2.6.2.2	RLC filter . . . . .	22
2.6.3	Converter side filter . . . . .	23
2.6.3.1	Filter return-connected to DC-link . . . . .	23
2.6.3.2	LCR Filter grounded . . . . .	24
<b>3</b>	<b>Method</b>	<b>25</b>
3.1	Modeling . . . . .	25
3.1.1	Cable . . . . .	25
3.1.1.1	Example of $\pi$ -section of cable . . . . .	26
3.1.1.2	Transient model for simulations . . . . .	27
3.1.2	Generator . . . . .	27
3.1.3	Inverter model . . . . .	29
3.1.4	PWM generation . . . . .	33
3.1.5	The filters . . . . .	33
3.2	Simulations . . . . .	34
3.2.1	Simulation circuits . . . . .	35
3.3	Validation of model through simulations . . . . .	37
3.3.1	Bandwidth . . . . .	37
3.3.2	Wave propagation . . . . .	37
3.3.3	Accuracy of LTspice . . . . .	38
<b>4</b>	<b>Results</b>	<b>39</b>
4.1	Overvoltage dependancy . . . . .	39
4.1.1	Risetime and cable length . . . . .	39
4.1.2	Frequency dependency . . . . .	41
4.1.3	Damping of the overvoltage . . . . .	43
4.2	Multilevel PWM for 1-phase simulations . . . . .	44
4.3	3-phase simulations . . . . .	44
4.3.1	FFT analysis . . . . .	46
4.4	A more realistic case . . . . .	48
4.4.1	Filter design and implementation . . . . .	48
4.4.2	FFT analysis . . . . .	51
4.4.3	Reducing filter size . . . . .	52
<b>5</b>	<b>Discussion</b>	<b>55</b>
5.1	Findings . . . . .	55
5.1.1	Possible other solutions . . . . .	55
5.1.2	Practical use of the results . . . . .	56
5.2	Limits of results . . . . .	56
5.2.1	Simulation . . . . .	57
5.2.2	Sensitivity of component parameters . . . . .	57
5.3	Environmental and ethical aspects . . . . .	57
5.3.1	Environmental . . . . .	57
5.3.2	Ethical . . . . .	58

<b>6 Conclusion</b>	<b>59</b>
6.1 Future work . . . . .	59



# List of Figures

1.1	Concept of Deep Green, underwater kite for production of tidal power. . . . .	1
1.2	A drawing showing the scope in the PTO. . . . .	3
2.1	2-level PWM switching. The blue sawtooth waveform represent the carrier waveform, the red waveform represent the reference signal and the PWM waveform is the resulting waveform when the carrier and reference waveform have been compared. . . . .	10
2.2	3 and 5 level PWM with 10ns risetime. . . . .	11
2.3	The two port $\pi$ -network for link $i$ . . . . .	12
2.4	The figure shows how the $\pi$ -section are constructed and how the different component parameters are defined. . . . .	15
2.5	The figure shows the reflection that occurs when there is a mismatch in impedance between two components in an electrical system. . . . .	16
2.6	The figure shows a voltage wave that is reflected at one side and continue travel back a forth between two joints of different impedances. . . . .	17
2.7	An overview of the filters that have been studied. . . . .	20
2.8	The figure shows the schematic of the RC and CRL filter, both are shunt connected at the generator terminal to reduce the reflection. . . . .	22
3.1	The circuit diagram of the generator for one phase . . . . .	28
3.2	The circuit diagram for all three phases of the generator . . . . .	28
3.3	Inverter topology for the 2 level switch, where each switch consist of 4 switches to be able to handle the voltage level over the switch. The three switches are assumed to switch simultaneously. . . . .	31
3.4	The figure shows the inverter topology for the 3 level inverter. Each switch in this case consist of two switches to be able to handle the voltage over the switch. . . . .	31
3.5	The figure shows the inverter topology for the 5 level inverter. Where the voltage over each switch is low enough to be handled by one switch. The 5 level inverter reduce the amplitude of the pulses and thereby the $dv/dt$ of the voltage. . . . .	32
3.6	The figure shows how the risetime is kept constant for each level of the inverters while the applied voltage is reduced and thereby lower the $dv/dt$ of the pulse. . . . .	32
3.7	Filter topologies for inverter side LCR filter . . . . .	34
3.8	4 $\pi$ -sections vs 100 $\pi$ -sections zoomed in on one switch. It can be seen that the simulation with 72 $\pi$ -sections have a higher bandwidth and will therefore be more accurate. . . . .	35
3.9	Schematic of the three phase system from the Simulation. . . . .	36

3.10 Reflection of one pulse being sent towards the generator over a long transmission cable rated for 3.3/4.2 kV. The figure shows the time it takes for the wave to reach the other side of the cable and the time it takes for the wave to be reflected propagate back and forth and return to the generator. . . . . 38

4.1 In Figure (a) voltage dependency on dv/dt is shown and in (b) a zoomed part of the graph is shown. . . . . 40

4.2 In (a) voltage dependency on dv/dt is shown and in Figure (b) a zoomed part of the graph is shown. . . . . 40

4.3 Voltage depending on cable length is shown for 400V (a) and 2800V in (b). . . . 41

4.4 Voltage pulses interfering with each other and thereby creating a higher voltage. The red curve is the PWM of the input voltage with a decreasing space of the negative part of the pulse. The blue curve is the voltage at the generator terminal which is increased when the pulses becomes shorter. . . . . 42

4.5 Voltage compared to the switching frequency, which shows that the voltage increase almost linear to the increasing frequency. . . . . 42

4.6 The figures shows the voltage at the generator terminal due to reflections. It can be seen that if the  $dv/dt$  is larger it also takes longer time for the reflections to be damped. . . . . 43

4.7 3-phase simulation for 2-level PWM. . . . . 45

4.8 FFT for the 3 phase cases with  $500kV/\mu s$  for different topologies for the inverter. 47

4.9 Waveform of the voltage with filter implemented. The red curve at the bottom is the voltage from the inverter, blue waveform is the voltage after the filter and the top red curve is the generator terminal voltage. . . . . 49

4.10 Waveform of the voltage for the realistic case after 5-level converter and the filter have been implemented . . . . . 51

4.11 The Figure shows 5-level PWM with a  $dv/dt$  of  $12.5kV/\mu s$  . . . . . 52

# List of Tables

3.1	Parameters of the chosen 3.3/4.2 kV cable from Nexans . . . . .	26
3.2	The table shows two examples of the parameters for the $\pi$ -model for up to 10MHz for 100m and 500m at a voltage level of 2.8 kV. . . . .	27
3.3	Parameters of the two different generators, 400V and 2.8kV . . . . .	29
3.4	The table shows the specifications of the chosen IGBT switch. . . . .	30
3.5	The table shows the velocity of the wave in the cable and the calculated and simulated time it takes for the wave to travel over the cable. . . . .	37
4.1	Difference in voltage between 2, 3 and 5 level PWM on a 1 phase system with a cable length of 100m. . . . .	44
4.2	Difference in voltage between 2, 3 and 5 level PWM on a 3 phase system rated for 2800 $V_{RMS}$ with a cable length of 100m and 72 $\pi$ -sections. . . . .	45
4.3	Difference in voltage between 2-, 3- and 5 level PWM for inverters with the same DC-link voltage of 5kV. The simulations are made on a 3 phase system, 100m cable, 72 $\pi$ -sections and the generator rated for 2.8kV. . . . .	48
4.4	Difference in voltage between implementation of different filters, 2-level PWM, 100ns risetime, 2.8kV LL, damping ratio of 1.45. . . . .	50
4.5	Difference in voltage between implementation of different filters, 3-level PWM, 100ns risetime 2.8kV LL, damping ratio of 1.45. . . . .	50
4.6	Difference in voltage between implementation of different filters, 5-level PWM, 100ns risetime 2.8kV LL, damping ratio of 1.45. . . . .	50
4.7	New values of the capacitor to keep overvoltages at 20% of the DC-link. The inductance and resistance are kept constant. The simulation is for a cable of 100m and 5-level PWM with 100ns risetime and 2.8kV line-line. . . . .	53
4.8	The tables shows how the value of the capacitance in the filter need to be adjusted when the inductance is reduced while keeping voltage level below 6kV line-to-line. . . . .	53
4.9	Reduction of resistance while keeping line-to-line voltage below 6kV . . . . .	53



# 1

## Introduction

### 1.1 Background

The desire for renewable resources for electric power generation has increased which makes the efficient utilization of the available resources of high importance. A resource that has not been widely exploited so far is the marine energy, which is found in the tidal and ocean currents. Every day the tides move large amounts of water that carries a lot of kinetic energy that can be used for energy production. The velocity of the tides is relatively slow making it difficult to generate power with existing technology. By using a moving kite with a wing, such as in Fig 1.1, that generates lift from the moving water the relative speed of the water moving past the power plant can be increased.



*Figure 1.1:* Concept of Deep Green, underwater kite for production of tidal power.

With the increased speed of the water through the turbine the potential for generating power is increased, thereby increasing the range of usable water speeds, such as slow tidal streams [1]. The tides depend on the position of the moon, the position of the sun and earths rotation. These factors decides when the tides are high and low. This makes the tides simple in

their nature and also makes them very predictable [2]. The predictability is a desired characteristic in a renewable resource, which results in a reliable and predictable energy production. Compared to many other renewable resources such as wind and solar the resource of tidal or ocean currents can provide stability to weak grids through predictive energy production.

Unfortunately there are several challenges with having power plants out in the open sea, one of which is the need to transmit the energy produced from the power plant. This requires the use of long cables that connect the power plant to the grid or the consumer. Along with long cables there are some characteristics that are undesired such as losses in the cable, harmonics and transients interfering with the system [3], [4]. By having the power plant under water at least some of the components of the plant needs to be submerged out at sea. This fact sets requirements on the system and the included components. The power plant is moving and therefore the components need to be as small and lightweight as possible while still providing all the electrical requirements for power production. That is why it is preferable to move as much of the needed components of the power plant out of the kite itself to a location that is not moving with the kite. Because of the need for components with high power density having a permanent magnet synchronous generator (PMSG) is required. To control a variable speed PMSG a pulse width modulated (PWM) inverter is needed in order to use maximum power point tracking (MPPT). The inverter controls the generator by controlling the torque and thereby the speed and power of the generator [5]. By having a PWM inverter connected with a long cable the problem with traveling waves and reflections presents itself [4]. PWM controlled machines with long cables have had a history of having breakdowns in the insulation of the machine due to high overvoltages caused by reflections in the power cable. Some of the reasons to the breakdown are: voltage at the inverter, risetime from the inverter, cable length between the generator and inverter and the generator insulation [6].

It is highly beneficial to minimize the risetime of these PWM inverters, since it is then possible to reduce the switching losses of the power switches. The short risetime of the power switches is one of the major factors in the overvoltage phenomenon due to reflections. One complication in this is the dilemma of having as fast risetimes as possible while at the same time mitigating the problem of overvoltages at the generator terminals. In the last couple of years a new technology has emerged as a viable option for having converters with lower switching losses than the existing converters have today. This technology is the widebandgap semiconductors, such as the SiC and GaN MOSFETs, which can have much faster risetimes than the existing IGBTs commonly used in applications today. Unfortunately this will result in even higher overvoltages which would damage and break electric machines if not treated properly. As of today some of the converters on the market operates with risetimes resulting in voltage steps of about  $5 - 6kV/\mu s$ , which does not utilize fully the capability of the newest power switches. This is most likely to increase in the near future with the ongoing research and results.

With the implementation of long cables in the electric drive system there is also a possibility to arrange the electric components in the most suitable configuration available. When doing this one needs to see what impact the long cables have on the system and analyze this in order to minimize electric losses and the negative effects in the transmission. This aspect is

what this masters thesis is going to focus on.

## 1.2 Aim

The aim of this Master's thesis is to study the effects of using long cables in an electric drive for a permanent magnet synchronous generator (PMSG) in a sub sea tidal power plant. The goal is to evaluate the problematic of a long transmission cable in the electric drive, from the inverter to the generator, given the design of the system and find possible solutions to these problems.

## 1.3 Scope

The focus of this project is to study the effects of long cables and their location for a complete electrical power take off (PTO) system. Different lengths of the cable and different components and topologies of the electric drive will be examined. The objective of the project is to study challenges for the system and to find solutions to the problems. One PTO system is in this project regarded as a generator, a back-to-back AC/DC and DC/AC converter, a filter and long transmission cables which consists of a cable in the tether of the kite and a cable on the sea bottom. The cable on the sea bed is connected to a point of common connection (PCC) that connects the power plant to the grid through a long high voltage cable. In this project the components up to the converter will be studied as indicated by the red rectangle in Fig 1.2.

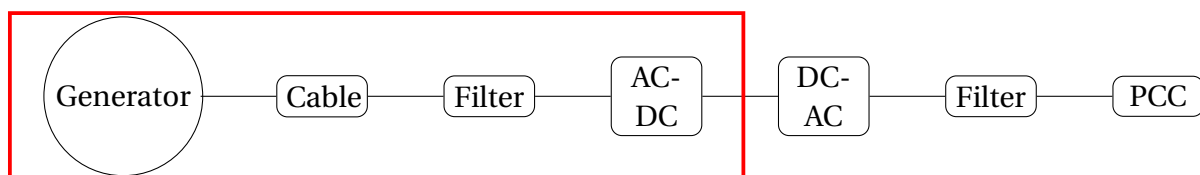


**Figure 1.2:** A drawing showing the scope in the PTO.

The configuration will only include one PTO and not an array of several PTOs working together, which would be a natural case for commercial production. The generator that was used in this project was a PMSG and variable speed, being controlled by a three-phase inverter. The requirements of the system are operation in a sub sea environment down to a depth of at least 100 m; located up to 1 km from the point of common connection; producing 100 kW of electrical power.

The effects of different voltage levels on the system will be investigated. The voltages in focus are 400  $V_{RMS}$  and 2800  $V_{RMS}$  as the voltage over the long cable. The electrical components were reduced to simplified versions for the simulations in order to keep the focus on the problems of the system. The inverter was reduced to a generated PWM signal and the generator was assumed to have a constant impedance.

Most commonly, when designing an electric power cable the international and national standards and regulations are used [7]. In this project, since the focus is not on designing a

power cable or components but the effects of different configurations of the system a typical cable for the application was used from a manufacturer where the parameters of the cable were known. The system was modeled in LTspice where different aspects and phenomena were considered, such as harmonics, reflections, overvoltages and transients. A simplification that was made is that the mutual inductance and capacitance between the phases were not considered, the cable is therefore seen as having three conductors individually shielded by a grounded shield.

The mechanical stress due to the movements of the kite on the different parts of the system was not taken into consideration. The maintenance of the system was not considered either. However, the study will review the different solutions and the results of the simulation regarding possible change in lifetime expectancy. The system should not need any maintenance due to overvoltages that damaging the components or the insulation of the cables. The loading of the machine affects the overvoltage, however, it is not well documented and will therefore not be of any focus in this project [8].

The voltage and its characteristic have been analyzed. The system has been analyzed as having voltage transients in the steady state operation and thus the voltage magnitudes have been in focus. Neither the active, nor the reactive power generated from the PMSG have been the focus of this study. If the voltage is within limits the current is assumed to be within limits as well. The voltage is seen as acceptable when the overvoltages of the line to line voltage has less than a  $\Delta V_{LL} \leq 20\%$  of the expected PWM voltage.

### 1.4 Task

The project has, through literature studies and simulations, examined problems that could occur during operation such as transient waves and harmonics and if a filter implementation could mitigate the overvoltages. In order to do so the system has been evaluated as having transient voltages. Little regard has been given to the fundamental frequency since it does not affect the high frequencies nor the overvoltages.

The electric power system of a power plant needs several components that need to function together for the system to be efficient and work properly. The components are usually the same for one type of power plant. One thing that can differ a lot is the control strategies [9], [10]. However, since the system in this report is a generic one the control strategy has been neglected. The importance in this report is in the connections of the different components and how the parameters of these affect the voltage.

The task is to mitigate overvoltages to a maximum of  $\Delta V_{LL} \leq 20\%$  at the generator terminals caused by the inverter switching and to analyze the effects of the parasitic components of the hardware. The maximum voltage that the generator can handle without causing faster aging of the machine windings insulation is decided by machine manufacturers. Since manufacturers usually have a buffer in the voltage magnitude to about 20% and this being the goal in some literature this has been the limit set as a goal for the voltage mitigation [11], [12].

# 2

## Theory

The power electric system of a power plant is the essential part of the PTO system to generate and transfer electrical power. The power electric system itself is made up of a few major components such as the generator, filter, cable and converter which are explained in this chapter.

### 2.1 System structure

The system structure of the PTO is as mentioned in the background and consists of the generator, transmission cable, filter and converter. Because of the unique situation of the power plant there system structure can be further described as having some more criteria. The generator needs to be as compact as possible with high power density. The mechanical power comes from the turbine moving trough water at different speeds due to the need for the kite to be moving in a figure of eight pattern, as can be seen in (2.1) the power that can be generated goes up with a power of three to the speed

$$P_{tide} = \frac{1}{2} \cdot \rho_{water} \cdot C_p(\alpha, \beta) \cdot A \cdot V_{current}^3 - P_{draglosses}. \quad (2.1)$$

The movements of the kite affect the generator and the other components, the kite should be designed with this in mind. The generator will be exposed to vibrations when the kite is moving. Because of this the airgap cannot be very small, some tolerance for some vibrations is required. Aspects such as this should be considered when choosing components to be used in an application like this.

In the trajectory of the figure of 8 the speed of the kite changes, with a change in the speed of the kite the water velocity through the turbine changes as well. This makes the use of a variable speed more suitable. Another part of the generator design that is set by the circumstances of having the generator in a moving power plant under water is the difficulty with grounding. The connection to ground in this type of moving power plant under water do not exist therefore the neutral of the generator is left electrically floating and the voltage in the neutral point is the common mode voltage.

The generator is controlled by an inverter. Due to the variable speed setup the generator needs to be controlled by a three phase AC/DC inverter. Depending on how and where the converter is located the concern for thermal development might present itself. Since all the components in the kite needs to be protected from the outside environment (the ocean) and from the vibrations of the kite the component can be needed to be packed in extra material,

however, this could be avoided by using the walls of the kite as a heat sink. The inverter itself can be controlled in a few different ways. The switching can be done in PWM or SVM pattern which affects the harmonics generated by the inverter. PWM switching generally has a higher switching frequency but also needs a higher DC voltage, unless a more advanced switching control is used that is called zero sequence injection. By using PWM the frequencies at the lower range is zero up to the switching frequency.

The filter that is required is dependent on the system requirements and the other components used. If the frequencies that needs to be taken care of is in the low frequency range the filter components need to be bigger. If the system requires that the voltage is perfectly sinusoidal the filter will have to be bigger than if the tolerances are not so tough. Depending on what voltages is being the focus of the filter the topology should be taken into consideration.

The transmission cable of a submerged power plant has a lot of similarities to a transmission cable that is designed for normal land based use. The sub sea cable need armoring, which the land based cable doesn't. The armoring makes the cable bigger and heavier. The parameters of sub sea cables are usually a bit larger than for the land based cables. Depending on the configuration there might be need for the power plant to have a conductor in the cable designated for the neutral/ground that is separate from protective ground.

### 2.1.1 System voltages

In the system and over the transmission cable the voltage can be divided up into two parts. The differential mode voltage and the common mode voltage. The combination of these two will be the resulting voltage [13]. In a system which is electrically floating the voltage of any point in the system is relatively arbitrary. The voltage potential can only be seen as having a different or the same voltage as another point in the system. With a floating system the voltage reference is not naturally ground since the components are not electrically grounded. This makes the natural point of reference of a phase another phase. The only connection to ground in a floating system is the stray capacitance to ground through the insulating material which usually is only affecting the system in high frequencies.

The differential mode voltage is a voltage that can be seen as the difference in instantaneous potential between the phases. When the inverter switches, the phases goes in and out of sync with each other, a difference in instantaneous line-to-line voltage arises

$$V_{diff_{AB}} = V_a - V_b. \quad (2.2)$$

The other differential voltages can be represented in the same way but for the other phases.

The common mode voltage, like the differential mode, arises from the inverter switching. Common mode voltage is the voltage from all of the three phases to ground [14]

$$V_{CM} = \frac{V_{aG} + V_{bG} + V_{cG}}{3}. \quad (2.3)$$

In a y-connected generator the y-connection has a finite impedance to ground, this coupling will have a high frequency current moving from the y-connection to the grounded outer shell

of the generator. This in turn implies that there is a voltage at the connection point. This voltage appears over a capacitive voltage divider that is the generator bearings where it will create discharges [15].

It is possible to reduce the common mode voltage by using the mutual inductance connection between the cable inductances and incorporate that in the filter [16]. However, by having individually shielded and grounded transmission cables this technology is not possible. Another problem with this voltage is the result of bearing currents that also wears down the generator and reduces its lifetime [16]. Together with this the neutral point voltage induces high frequency voltage in the shaft of the generator and induces a current to ground through stray capacitances. This current has shown to interfere with ground fault protection systems [16].

## 2.2 Generator

To have a generator in an industrial plant there are several requirements that needs to be properly addressed for the plant to be accepted to generate power for distribution [17]. For a power plant with high requirements on being compact and having high energy density a PMSG is suitable [18], [19]. Since a PMSG only has negligible losses in the rotor due to the absence of current in the rotor to generate the magnetic flux a PMSG can have a lower volume compared to an induction motor. Since the power plant is under water and moving there is a need for the generator to be as compact as possible with the highest power density possible. When high energy density is needed a machine with permanent magnets is preferable. With no heat dissipation from the rotor the machine can withstand a higher power rating compared to if there were losses in the rotor as well. Resulting in PMSG being more power dense [20].

The model of the PMSG is the same as for a synchronous generator [21]. Usually the machine is modeled for the fundamental frequency and it is simplified to the extent that the capacitive parasitic effects can be neglected. In the case of transients this model is insufficient in representing the machine. Therefore a capacitive element, the stray capacitance  $C_s$  is introduced that represent the capacitance between the windings and  $C_m$  to the grounded stator frame. The equivalent schematic of the generator literature says can be quite different from one machine to another. Depending on the design and the geometry of the machine the parasitic parameters will differ and with that also the equivalent schematic. The most accurate way of extracting the equivalent circuit for the generator is to measure the parameters over the frequency bandwidth of interest and match those values in the model [14], [22]. In general, for a medium voltage generator one can say that a larger generator has lower parameters [23].

### 2.2.1 PMSG

There are a few different ways of designing a PMSG. One of the aspects to consider is how to attach the permanent magnets to the rotor. Gluing them to the outside of a round rotor, surface mounted PM, or having them embedded into the rotor, insert-mounted PMs. In this project the assumption has been made that the PMSG used in the model is of the former. This results in the inductance of the PMSG is constant regardless how the rotor is positioned,  $L_s = L_d = L_q$ .

### 2.2.2 Variable speed

In a system which is moving and has changes in water flow through the turbine, the use of a variable speed generator is preferable. A variable speed PMSG has a more even power production due to the possibility to change the torque of the generator as the speed changes. With variable speed the power plant has more constant torque which results in a longer lifetime. The constant speed has slightly higher efficiency but the variable speed solution is more economic when considering the lifetime [24], [25]. Along with variable speed short-time flicker is present, this can be mitigated by controlling the converters [26].

### 2.2.3 Problems with overvoltage

If the windings in the stator are exposed to higher voltages than designed for, the insulation of the winding will break and short circuit. To secure the generator the insulation could be made to withstand a higher voltage, however, it is not common practice. The generator has a certain maximum voltage that is allowed before it breaks [27], [28], [29], [30].

Depending on how the windings of the generator are wound there will be some difference in how high and how fast voltage it can withstand [31]. When a voltage pulse arrives at the generator terminal the entire winding will not have the pulse evenly distributed over it instantly. It takes some time for the voltage pulse to travel across the winding. If the pulse is very steep just the first few turns of the winding will have all of the voltage across them and is therefore in a higher risk of having hastened aging or breakdown. In addition to one pulse being steep, if the windings are wound with two phases in one slot, or both, the winding can have the full line to line voltage over a few of the first turns. If the windings insulation is not enough to withstand the voltage the insulation will have a hastened aging [32], [33].

If the voltage is too high there might even be coronas, that will break down the insulation [34]. Stress relief coatings are one of the tools used to increase the toughness of the generator against overvoltages [35]. Above about 1kV the electrical stress is the main aspect of consideration when designing the insulation, below that the mechanical stress is the main factor to consider. Below a certain voltage that the generator is designed for there is practically no aging [35].

## 2.3 Power electronic converters

For a PMSG the inverter is in charge of the control of the power transfer. An inverter is a converter that by semiconductor switching controls the voltage and current of an electrical power generating unit. In this project this unit is the PMSG. There are a few different control methods to control a variable speed PMSG when using inverters [36]. One is to control the inverter output voltage by controlling the switching of the inverter in a PWM pattern.

The use of PWM converters are known to cause high frequency disturbances in the system, especially when they are connected to a long cable that transmits the power [6], [37]. This leads to conducted electromagnetic interference (EMI) given by the parasitic elements of the cable when exposed to steep voltages. Common mode as well as differential mode voltages creates electromagnetic interference in the electric system. Which needs to be mitigated in order to achieve good power quality.

### 2.3.1 PWM switching

The PWM switching is essential to this kind of generator control. By having a high switching frequency the EMI and switching harmonics can be moved to higher frequencies and reduce the needed size for the filters [38]. However, with a higher frequency the need to mitigate the overvoltages is even more important. Due to high switching frequency the overvoltage will be increased due to more pulses interacting with each other [39], [40].

The switch consist of a gatedriver-integrated circuit (G-IC), resistor and the IGBT. The switching is controlled by the G-IC and the resistor controls the risetime of the switching voltage. The voltage that is applied to the switch is the voltage that create output voltage. By using the same G-IC and resistor at the gate of the IGBT means that the risetime of the gate voltage,  $V_{gs}$  is the same risetime that the applied voltage of the switch have,  $V_{ds}$ . By having the same risetime independent of the voltage applied means that the  $kV/\mu s$  will decrease when a higher number of voltage levels in the PWM are used or when the voltage applied to the switch is lower.

The phase amplitude depends on the the modulation ratio and the DC-Link voltage. The control wave is compared to the triangular wave and depending if the control voltage is larger or smaller than the triangular waveform certain switches are open or closed. It is the frequency of the triangular waveform that is the switching frequency. The ratio between the amplitude of the control wave and the triangular wave can be described as

$$m_a = \frac{\hat{V}_{control}}{\hat{V}_{tri}} \quad (2.4)$$

where  $m_a$  is the amplitude modulation ratio. The amplitude modulation ratio describe how long and often the switches will turn on and off. This will in turn determine the amplitude of the resulting sine wave of the PWM will have

$$V_{phase} = m_a \frac{V_d}{2} \quad (2.5)$$

where  $V_{phase}$  is the amplitude voltage of the phase.

## 2.3.2 Topology

For the multilevel PWM waveform several carrier waveforms are added for the three and five level PWM. For this two respectively four carriers are used to create the number of levels in the PWM signal that were needed for 3- and 5-level switching. When several carriers are used the voltage can switch in smaller steps and the resulting in a waveform which is more similar to a sine wave. Another positive aspect of having more levels in the switching is that the voltage does not have as high amplitude steps as for a two level converter.

### 2.3.2.1 2 level PWM

In a 2 level topology for a PWM inverter there is a DC-link and that DC-voltage is divided over two transistors that thereby can give the output either  $+V_{DC}/2$  or  $-V_{DC}/2$ . This result in a voltage step of  $|V_{DC}|$  with every switch, because both switches are controlled by the same signal. One of the switches is at any given time on and the other is off and they switch with a reference wave over a carry wave.

In the 2 level PWM inverter construction the voltage steps between  $-V_{DC}/2$  and  $+V_{DC}/2$  and is constructed as follows, the voltage output from the inverter is  $+V_{DC}/2$  when the carry signal is lesser than the reference and the output voltage is  $-V_{DC}/2$  when the carrier is larger than the reference, this is shown in Fig 2.1. The switching frequency is proportional to the switching of the carrier waveform.

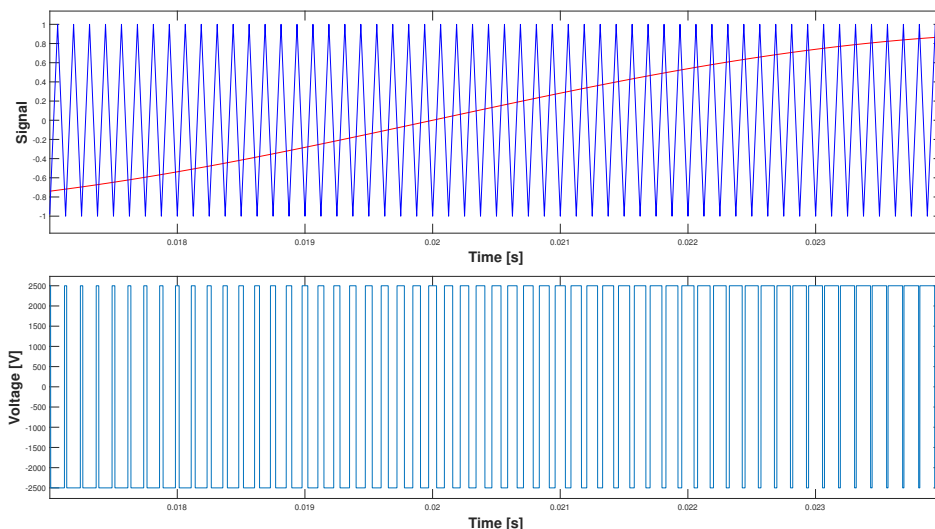
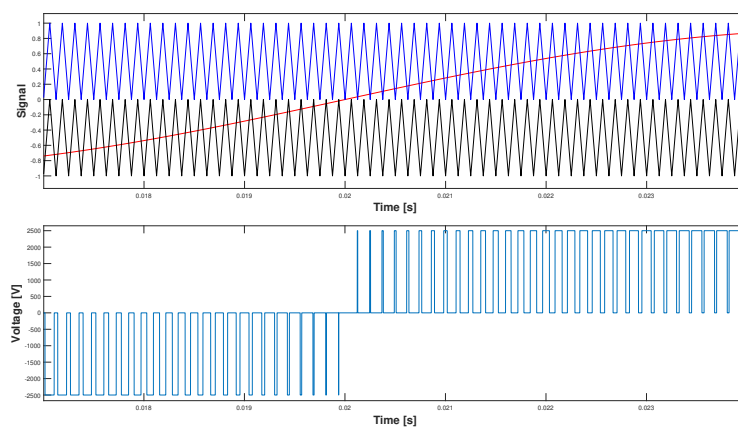


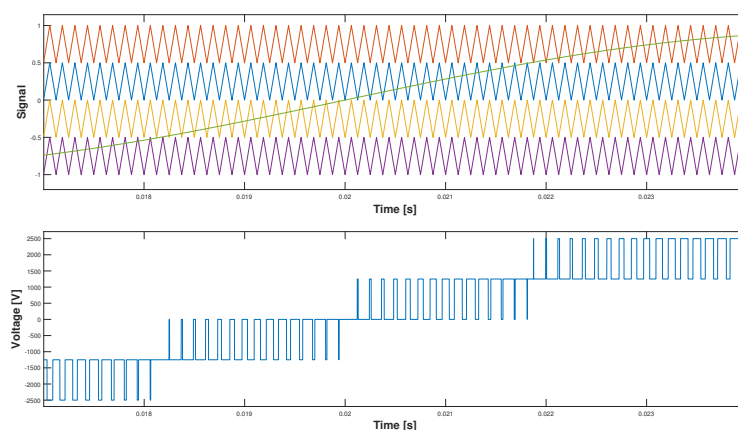
**Figure 2.1:** 2-level PWM switching. The blue sawtooth waveform represent the carrier waveform, the red waveform represent the reference signal and the PWM waveform is the resulting waveform when the carrier and reference waveform have been compared.

### 2.3.2.2 Multilevel PWM

Multilevel converters have more voltage steps than a 2-level converter. Instead of switching with a step of  $V_{DC}$  they switch with a reduced voltage step and can move between voltage steps to get a better representation of a sine wave as can be seen in Fig 2.2. By having the voltage step and  $dV/dt$  smaller the overvoltage at the generator becomes lower as well. Even though having smaller voltage steps in the inverter the overvoltages will not disappear [41]. The more levels a multilevel PWM topology has, the more complex the switching controls is. By having more voltage steps there is a need for more components which needs a more careful control.



(a) Generated 3 level PWM switching. A three level PWM has voltage steps of  $V_{DC}/2$ . The control strategy lets the voltage move between three levels:  $+V_{DC}/2$ ; 0 and  $-V_{DC}/2$ .



(b) Generated 5 level PWM switching. A five level PWM has voltage steps of  $V_{DC}/4$ . The control strategy lets the voltage move between five levels:  $+2V_{DC}/4$ ;  $+V_{DC}/4$ ; 0;  $-2V_{DC}/4$  and  $-V_{DC}/4$ .

**Figure 2.2:** 3 and 5 level PWM with 10ns risetime.

## 2.4 Submarine power cable

This section describes what defines a submarine power cable and its characteristics. How its parameters are found and some problems with them [7]. Submarine power cables are different than regular power cables that is commonly used on land. The differences have resulted in the requirement for a standard for planning, installing and design of such cables [42]. The primary difference between submarine cables and cables for land use is the armoring [43].

With the armoring the cable becomes bigger. The addition of materials affects the cables parameters. One thing that is increased is the dielectric losses. However, for such low voltages as  $2800 V_{AC}$  the dielectric losses can be neglected [7], [44]. One of the clear characteristics and problems with having long power cables is the power loss in the cable. This is wanted to be as small as possible. There can be, if the cable has metallic armoring, an induced current in the armoring of the cable that creates extra losses [45].

There are a few different models that can be used for transmission lines. The  $\pi$ -section is commonly used in modeling transmission systems of 50 or 60 Hz. This can be divided up into lumped parameter model and distributed parameter model. Lumped parameter model is the most simple one. As the name suggests the parameters of the cable are lumped and are represented by one element. The distributed model have the parameters of the cable distributed over several elements. This is used when there are changes in the voltage over the distance of the transmission line, such as transients, fast voltage switchings or voltages with high frequencies such as square waveforms such as PWM.

In power systems, to model a transmission line one can use short, medium or long line model for  $<80\text{km}$ ,  $80\text{-}250\text{km}$  and  $>250\text{km}$  respectively. The medium and short line model uses lumped parameters for the total impedance and the shunt capacitance is considered lumped at each end of the line as in Fig 2.3. For transmission lines longer than  $250\text{km}$  the distributed parameter model must be considered for an more accurate solution, which means that several  $\pi$ -sections are used to model the cable [46]. The same can be done for high frequency models. The real cable can be seen to have an infinite number of  $\pi$ -sections but to model the cable a definite number of  $\pi$ -sections are used. The total impedance of the cable is evenly distributed among the  $\pi$ -sections which creates an approximation of the real cable.

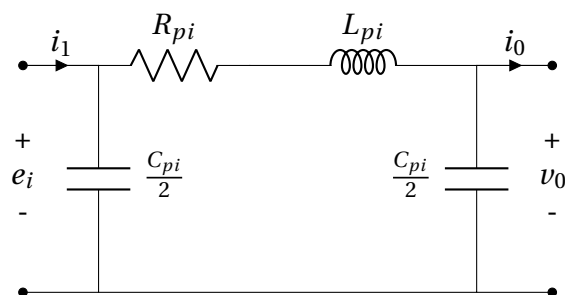


**Figure 2.3:** The two port  $\pi$ -network for link  $i$ .

When modelling transmission lines for high frequency voltages these models lack the properties to show the changes in the parameters that occurs as the frequency changes. At higher

frequencies the skin effect and proximity effect changes the value of the resistance. This change cannot be accurately modeled with these models. One way of extending the model to incorporate the change is to model the resistance as an RL-ladder [47]. By modeling the parameter as a ladder the effective resistance changes with the change of frequency, same for the reactive parameters. The other alternative is to estimate the parameters for one frequency and approximate the parameters to that one frequency.

### 2.4.1 Parameters and characteristics of a submarine cable

The main aspect to consider is the capability of the cable to withstand the heat that is generated by the current flowing in the cable. With the heat generated by the current flowing in the cable there is a change in the resistance. A cable with a higher operating temperature has a higher resistance which can be calculated as

$$R_{DC'T} = R_{DC'20}[1 + \alpha_{20}(T - 20)] \quad (2.6)$$

where  $\alpha_{20} = 3.93 * 10^{-3} [K^{-1}]$  for copper and  $T$  is the operating temperature. The manufacturer writes in the datasheet the standard parameter and the operating resistance for the cable is calculated using (2.6). The thermal resistances and the effects of the thermal increase in the cable during operation can possibly be a factor that changes and thereby changes the resistance of the cable [48].

The parameters that are being used in the modeling of a transmission cable are R (resistance), L (inductance), C (capacitance) and G (conductance), in this case the conductance is neglected since it is very small. The parasitic effects of a cable are shown throughout the frequency spectrum and changes depending on the frequency [3], [49]. At low frequencies the resistive parts are dominant. Depending on what frequency it is the dominant part of the cables parasitic effect might change. It seems that for medium to high frequencies, up to about 70 kHz the inductive part is dominant, with the  $L_{DM}$ . At very high frequencies the capacitive part becomes more dominant.

### 2.4.2 Frequency dependency

A well known effect on the parameters of a cable with the change of frequency is the skin effect. At high frequencies the resistance of the cable increases.

Another effect is the proximity effect in bundled conductors. For high frequencies the currents in the conductors tend to flow on the side facing the neighbour conductor. That results in further increase in resistance. If the currents of the conductors are flowing in opposite directions, the inductance is decreased as well. Capacitances decrease with increasing frequency. This because of the polarization of the dielectric. These effects are shown well for high frequencies, 1kHz and up. However, the inductance can change significantly with harmonics.

These frequency dependent effects are present in the system and will affect the parameters. However, the effect that is active will be small due to the fact that there is a low energy content in these high frequencies for a power generating system.

### 2.4.2.1 Skin effect and proximity effect

The resistance of an AC conductor is dependent on the frequency of which it operates. When the frequency increase so does the resistance. The reason is that the current flows more in the outer parts of the conductor resulting in a smaller conducting area.

$$R_{AC} = R_{DC}(1 + y_s + y_p) \quad (2.7)$$

Where  $R_{AC}$  is the resistance of the conductor for a given frequency. Here  $y_s$  is the skin effect and  $y_p$  is the proximity effect which are given by

$$y_s = \frac{x_s^4}{192 + 0.8x_s^4} \quad (2.8)$$

where the factor  $x_s^4$  is

$$x_s^2 = \frac{8\pi f}{R_{DC}} k_s * 10^{-7} \quad (2.9)$$

where  $k_s$  is equal to one for a equilateral triangular placed cable. The factor for the proximity effect is

$$y_p = \frac{x_p^4}{192 + 0.8x_p^4} \left( \frac{d_c}{s} \right)^2 \left[ 0.312 \left( \frac{d_c}{s} \right)^2 + \frac{1.18}{\frac{x_p^4}{192 + 0.8x_p^4} + 0.27} \right]. \quad (2.10)$$

Here the  $d_c$  is the diameter of the conductor in [mm],  $s$  is the distance between the center of the cables and the factor  $x_p$  is

$$x_p^2 = \frac{8\pi f}{R_{DC}} k_p * 10^{-7} \quad (2.11)$$

where  $k_p$  is 1 for a non-impregnated cable. These equations describe the increase in resistance that comes at higher frequencies than DC [50].

### 2.4.2.2 Hyperbolic correction

The voltage in the system has a wide frequency spectra which consists of several other frequency components than 50 Hz. In the data sheet the values of the components are valid for a frequency of 50 Hz but due to the frequency dependency of the components the altering frequency change the values of the components and therefore a hyperbolic correction is needed to correct the value of the components. The frequency at which the hyperbolic correction is preformed means that the parameters of the  $\pi$ -section is the most accurate at the frequency where the hyperbolic correction is preformed. The impedance and the admittance of the cable is described by

$$Z = R + j\omega L \quad Y = G + j\omega C \quad (2.12)$$

where the conductance  $G$  is neglected. The parameter  $\omega$  is the frequency where the hyperbolic correction is preformed and where the value of the components are most accurate. The impedance and the admittance describes the surge impedance  $Z_C$  of the cable

$$Z_C = \sqrt{\frac{R + j\omega L}{j\omega C}} = \sqrt{\frac{Z}{Y}} \quad (2.13)$$

and the propagation constant  $\gamma$

$$\gamma = \sqrt{(R + j\omega L)(j\omega C)} = \sqrt{Z \cdot Y} \quad (2.14)$$

This gives the impedance  $Z'$  for each  $\pi$ -section

$$Z' = Z_C \cdot \sinh\left(\frac{\gamma l_C}{N_\pi}\right) \quad (2.15)$$

and  $Y'$  is the admittance per  $\pi$ -section

$$\frac{Y'}{2} = \frac{1}{Z_C} \tanh\frac{\gamma l_C}{2 \cdot N_\pi} \quad (2.16)$$

in (2.15) and (2.16) is  $l_C$  the length of the cable and  $N_{\pi i}$  is the number of  $\pi$ -section that are used in the model. For each  $\pi$ -section the resistance, inductance and capacitance are calculated as

$$R_\pi = \text{real}(Z') \quad L_\pi = \frac{\text{imag}(Z')}{\omega} \quad C_\pi = \frac{\text{imag}(Y')}{\omega} \quad (2.17)$$

The value for each component is inserted into the model for the  $\pi$ -sections as can be seen in Fig. 2.4 [11].

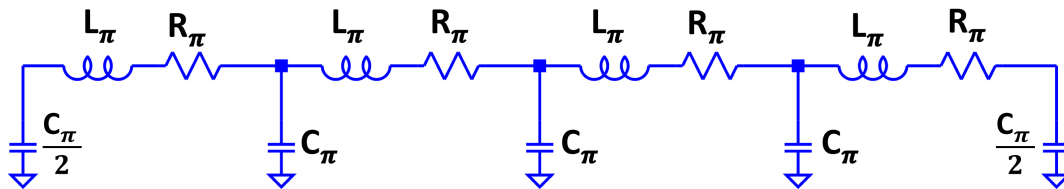


**Figure 2.4:** The figure shows how the  $\pi$ -section are constructed and how the different component parameters are defined.

The number of  $\pi$ -sections represent the frequency spectra the model is accurate for by

$$N_\pi = \frac{8 \cdot l_C \cdot f_{max}}{v_C} \quad (2.18)$$

where  $N_\pi$  is the number of  $\pi$ -sections,  $l_C$  is the cable length,  $v_C$  is the speed of the traveling waves and  $f_{max}$  is the approximated frequency range that is represented by the model [51].

### 2.4.2.3 Shielding

The shielding of the current is needed to keep the electromagnetic field inside the cable. With a grounded shield around the conductor the electromagnetic field will not interact with anything outside of the cable. Depending of how the shielding is constructed the cable get a coupling capacitance between each phase [52], [53], [54]. If each phase is shielded separately the phases do not interact with each other.

## 2.5 Overvoltage due to wave propagation

When there is a voltage source in the system with fast risetimes of the voltage there is a risk of having reflections in that system. The magnitude of the reflection depends on the reflection coefficient which is represented by the impedance of the cross section between the components in the system. If there is an impedance mismatch between the components a reflection occurs, the larger impedance mismatch the larger reflection. As can be seen in Figure 2.5 if a voltage wave is travelling from  $Z_1$  towards  $Z_2$  an increase in voltage occurs at the mismatch if  $Z_1$  is larger than  $Z_2$  [55]. If the opposite case is true, when  $Z_1$  is less than  $Z_2$  a voltage decrease occurs [56], [57].

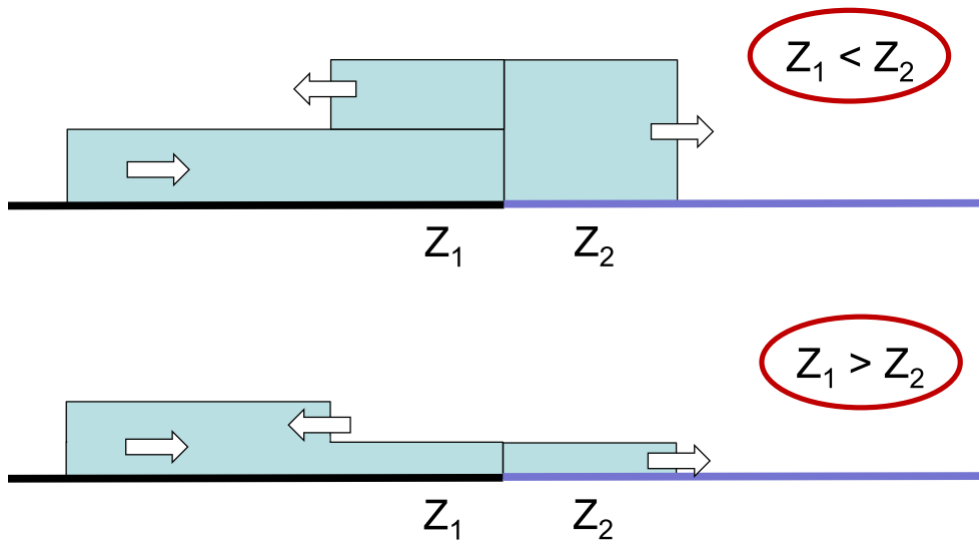


**Figure 2.5:** The figure shows the reflection that occurs when there is a mismatch in impedance between two components in an electrical system.

The reflection coefficient is represented as

$$\Gamma_n = \frac{Z_2 - Z_1}{Z_1 + Z_2} \quad (2.19)$$

where  $Z_1$  and  $Z_2$  represent the impedance of the component i.e. cable, generator or inverter. The voltage at generator and inverter are derived as an infinite sum of wave traveling back and forth [58]. When the wave hit the end of the cable where either the motor terminal or the inverter terminal is placed the voltage wave is reflected. The reflected wave then travels on the cable to the other side where it is reflected again, this can be seen in the lattice diagram in Fig. 2.6 [55].

Usually for electric motors the characteristic impedance is ten to hundred times higher than the characteristic impedance of the cable [59]. Typical reflection coefficient for a 125 hp (93kW) motor is 0.82 and for an inverter is 1 since it is completely stiff in the aspect of reflection [60]. The transmission coefficient

$$1 + \Gamma = \frac{Z_2 - Z_1}{Z_1 + Z_2} \quad (2.20)$$

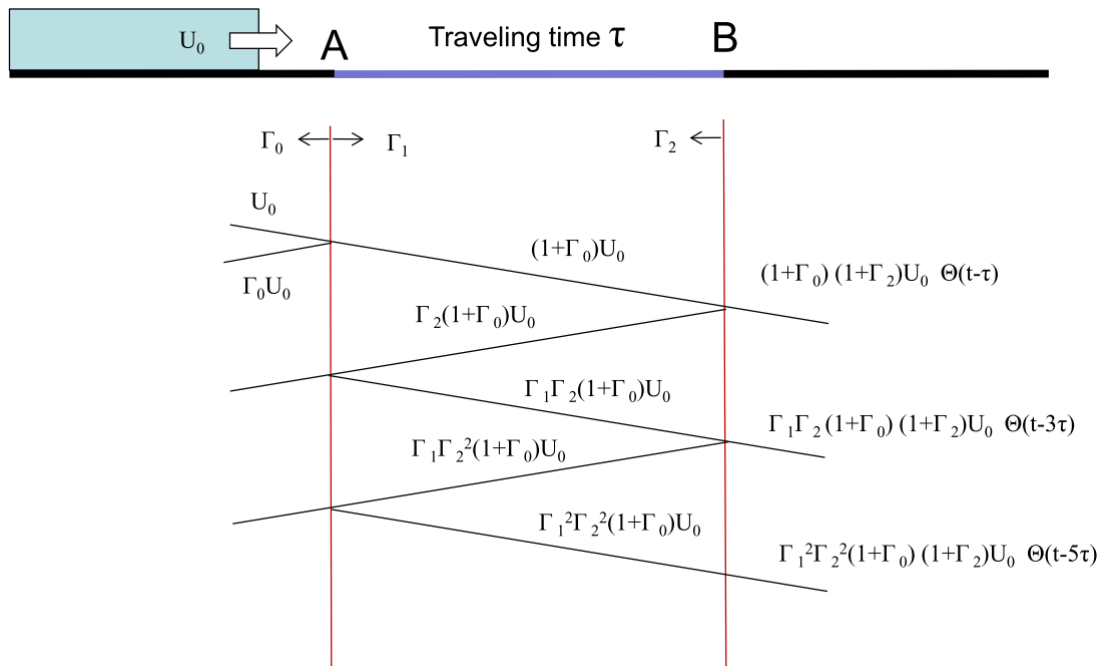


**Figure 2.6:** The figure shows a voltage wave that is reflected at one side and continue travel back a forth between two joints of different impedances.

which represent the amplitude or intensity that is being transmitted compared to the incoming wave [55]. If the risetime is shorter than three times the propagation time of the cable there will be reflections at the end of the cable, given there is an impedance mismatch [61].

### 2.5.1 Reflections

The aspects affecting reflected waves magnitude is [8]:

- Motor and cable surge impedance
- Cable length
- Magnitude of drive pulse
- Risetime of drive pulse
- Spacing of PWM pulses.
- Motor load

The phenomena of reflections in a transmission line cause overvoltages when the reflected wave moves over the transmission line and interacts with another voltage potential, the next PWM pulse for example [62]. An overvoltage is a voltage that is higher than the nominal operating voltage of the system. The peak voltage at the machine terminal can be described by

$$V_{peak} = \left( \frac{3\tau}{t_r} \cdot K_L + 1 \right) V_{DC}, t_r \geq 3\tau. \quad (2.21)$$

This shows that the risetime of the PWM pulse needs to be greater than  $3\tau$  in order to avoid voltage doubling [61].

A traveling wave is a function of the risetime of the voltage from the inverter and the length of the cable [63]. The wave also travels with approximately half of the speed of light [63]. The

speed of the traveling wave is a function of [52], [11]

$$v_C = \frac{1}{\sqrt{L_C \cdot C_C}} \quad (2.22)$$

where  $L_C$  and  $C_C$  are the distributed inductance and capacitance per unit length of the cable. The time for the wave to travel over the cable is therefore [52]

$$t_{travel} = \frac{l_C}{v_C} = l_C \cdot \sqrt{L_C \cdot C_C}. \quad (2.23)$$

It is possible to calculate the maximum allowed risetime of a pulse in order to keep it under a certain overvoltage [4].

$$t_r = \frac{4 * t_{travel}}{\delta V_{max,p.u.} + 1} \quad (2.24)$$

gives the maximum allowed risetime with reflection coefficients of 1, -1. However, for the distances of interest and a state-of-the-art inverter with fast risetimes of the switches this results in a relative large difference. The equation gives a result of approximately  $3\mu s$  for a 100m cable, compared to ca 10-100ns risetimes of a state-of-the-art inverter [8].

### 2.5.2 Risetime

When the risetime, or the voltage step is increased the overvoltage increases. At a reflection coefficient of  $\Gamma = 1$  the voltage step plus the reflection voltage will be the voltage at the point of reflection, in this case the generator terminal. This gives that a fast risetime have less time to be damped [8].

### 2.5.3 Frequency

When the frequency is increased the number of pulses for a given time increases as well. With pulses more often there is less time for each pulse to be damped out before the next pulse arrives. This results in that a higher frequency will have higher overvoltage [8].

### 2.5.4 DC magnitude

The higher the voltage step the higher the voltage plus of the reflection will be. Given a reflection coefficient of  $\Gamma = 1$  the voltage at the generator terminal will be the double of the DC magnitude [8].

### 2.5.5 Cable length or cable impedance

The length of the cable also affects the overvoltage up to a point. If the cable is very short, negligible short then there will not be any overvoltages due to reflections. On the other side the maximum overvoltage that the length of the cable can affect is up to two times the voltage step, a voltage doubling. Every system has a critical cable length, a length of the cable where the voltage gets doubled. It can be described through

$$l_c = c * \pi * t_{rise}[m] \quad (2.25)$$

where  $c$  is the speed of light and  $t_{rise}$  is the risetime of the pulse [8]. This shows that the critical cable length is dependent on other aspects of the system such as the risetime of the PWM pulses. The total impedance of the cable depends on the cable length.

### 2.5.6 System resonance

The reflections propagating back and forth on the cable can be seen as a frequency that resonates in the system. The sent input pulse at the inverter and the received pulse at the generator terminal has some time delay. The generator terminal first receives the voltage pulse which then is reflected back and forth and creates a new frequency in the system that is dependent on the systems characteristics.

This phenomenon is then extended to higher frequencies as well. The interference with the reflections and PWM pulses will, with the higher frequencies reflect several times and create several higher frequencies in the same way. This can be seen in an FFT of the generator terminals as strong peaks in 100kHz-MHz range, depending on the system characteristics as

$$f_{reflection} = \frac{1}{t_{travel} * 4}. \quad (2.26)$$

If the cable capacitance and inductance create a resonant circuit and overvoltages can be generated in the system [11], [64], [4]. If there is a voltage gain at a certain frequency this amplification will also appear at generator terminal, where the resonant peak appears depends on the components in the system [65]. The cable creates resonant peaks from the parasitic components, when adding a transformer or filter that changes the systems impedance the resonant frequencies change because they are dependent on the parameters of the system [65].

## 2.6 Filter

In order to improve the power quality and protect the system from overvoltage stress and ringing one can use different types of filters. Several different types of filters have been tested by a number of researchers [16], [66]. However, they prove that it is difficult to address both common mode and differential mode voltages with the same filter. Both in large systems with several generators being active at once and for small plants with just one generator, filters are needed [67]. One thing to keep in mind when generating power is the phase shift that comes with the introduction of filters [68]. In Fig. 2.7 an overview of the possible filters of the system is shown.

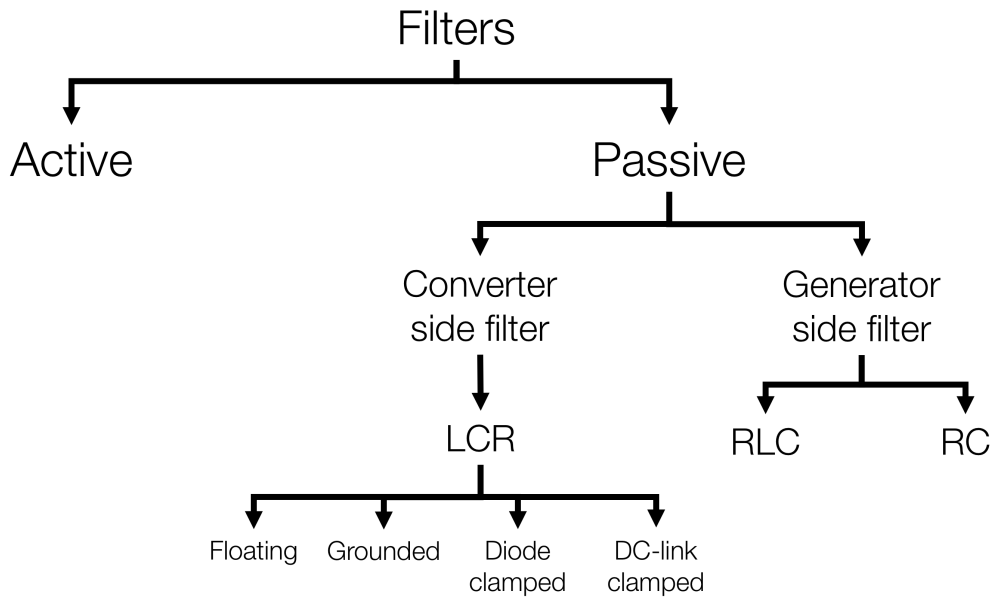


**Figure 2.7:** An overview of the filters that have been studied.

For a system with a PWM converter and a generator connected by a long cable a first order shunt filter connected at the machine terminals have been successful [63], [69], [70]. RC filters can be used at the motor terminal, this reduces the load impedance at high frequency. When connecting an RC filter at the generator terminal the reflection coefficient is changed, which by itself reduces the overvoltage through reflections. Another method is to connect an LCR filter to the inverter output, which has been shown to reduce the voltage overshoot by increasing the risetime of the pulse and filtering high frequency components [61]. When a filter is implemented at the inverter terminal it lengthens the risetime of the pulse to lower the voltage on the generator terminal [61]. The filters can be designed both on inverter side and the motor side by using the transfer functions [69].

### 2.6.1 Filter design

Filter design is an important part of making the system behave as wanted. The placement of the filter as well as the components and their parameters are all critical in order to mitigate the overvoltage [11].

There are different kinds of filters that can affect different parts of the signals. A  $dV/dt$  filter is made to increase the risetime of a voltage and smoothen out sharp edges in the waveform. A  $dV/dt$  filter is used to reduce the magnitude of high frequency component in the system. When designing the filter it is preferable to investigate the transfer function in order to get the required values [61].

There is also another type of filter, a sine filter. Which is used to improve the shape of a certain frequency to reduce the THD of the signal and make it more sinusoidal. These types of filters are used when there is a requirement on power quality, at a grid connection for example.

There are two categories, active and passive filters. Active filters use an active component, such as an OP-amplifier or switches. These filters are commonly not used for filtering in power generating units since they require power themselves [68]. The method of using active filters in motor drives is rarely used since it has some more requirements compared to passive filter, such as additional switches and complex algorithms [71]. They are also usually more expensive [27].

Passive filters can be built in many different ways. Depending on the filter configuration and the components used the filter will be effective against different aspects of the system. A passive filter that is connected in series needs to be able to withstand all the current going through the line. A shunt connected filter does not need the same requirement for current and can therefore be smaller. There are common mode filters and differential mode filters, and some that tries to mitigate both [66]. In order to mitigate the common mode voltage some use the mutual inductance of the cables and others have tried other methods such as reconnecting the y-connection of the filter with the inverter in different ways [66], [72], [73].

By connecting the three phases with a y-connection the differential mode voltage is affected. With a designed filter with filter parameters in an appropriate range, the differential mode voltage can be reduced to a desired limit.

In the system there exist both common mode and differential mode voltages. The common mode voltage, that is the combined voltage of all the three phases can not be mitigated by using common passive filters that are connected between the three phases.

## 2.6.2 Generator side filter

In this section filter design for filters placed at the generator terminal is presented.

### 2.6.2.1 RC filter

The RC filter have the purpose to match the impedance of the cable and the generator terminal. According to (2.19) the impedances should be the same in order to avoid a reflected voltage. This is solved by placing a module consisting of a resistor in series with a capacitor in parallel with the motor which is seen in Fig. 2.8 [11]. One module is connected to each phase and is Y-coupled between the phases. The resistance of the RC-filter is defined as

$$R_{RC} = \text{real}(Z_C) \quad (2.27)$$

where  $Z_C$  is the impedance of the cable. The resistor is thereby matched with the resistance of the cable and the reflection coefficient is reduced. The capacitance in the filter is added to improve the damping of the voltage at the generator [63]. The capacitance is calculated as

$$C_{RC} = \frac{(-1) \cdot 3 \cdot \left( l_c \cdot \sqrt{L_c \cdot C_c} \right)}{2 \cdot Z_C \cdot \ln(p)} \quad (2.28)$$

where  $L_C$  and  $C_C$  is the inductance and capacitance of the cable and p is the remaining part of the voltage that the filter should be designed for, p=0.8 in this case with 0.2 allowed

overvoltage [12]. The capacitor creates a short circuit at higher frequencies gives that there no impedance mismatch at the higher frequencies where the reflections are created due to the resistor that is matched to the characteristic impedance of the cable [12]. The total impedance of the filter therefore become

$$Z_{RC} = \left| R_{RC} + \frac{1}{j \cdot 2 \cdot \pi \cdot f \cdot C_{RC}} \right| \quad (2.29)$$

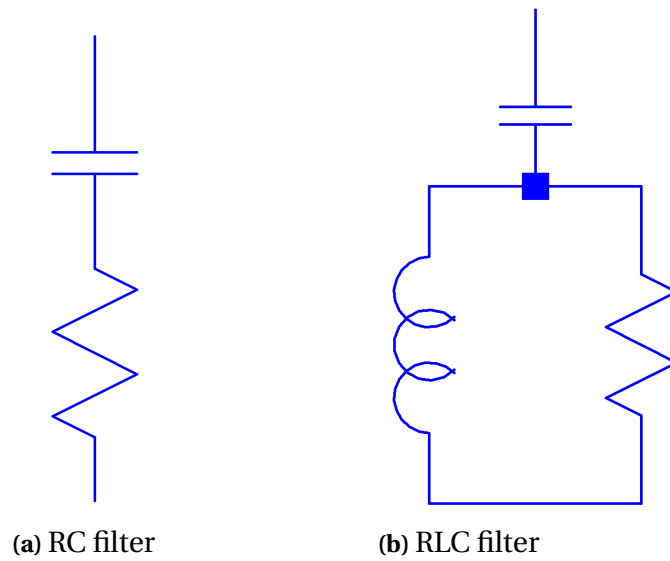


**Figure 2.8:** The figure shows the schematic of the RC and CRL filter, both are shunt connected at the generator terminal to reduce the reflection.

### 2.6.2.2 RLC filter

The RLC-filter can be implemented at the generator terminal in order to also match the impedance of the cable and the input impedance of the generator. The RLC filter is constructed as a capacitor in series with a parallel-connected inductance and resistor. That is placed at the generator terminal to mitigate the reflections, the schematics can be seen in Fig. 2.8(b) [11]. The components are designed with a set frequency tuning as follow, the resistance of the filter is matched against the resistance of the cable as

$$R_{RLC} = \text{real}(Z_C) \quad (2.30)$$

where  $Z_C$  is the impedance of the cable. The capacitive part of the filter

$$C_{RLC} = \frac{1}{2 \cdot R_{RLC}} \cdot \frac{1}{2 \cdot \pi \cdot f_{\text{tuned}}} \quad (2.31)$$

where  $f_{\text{tuned}}$  is the tuned frequency for the filter [11]. The inductance is

$$L_{RLC} = \frac{1}{C_{RLC}} \cdot \left( \frac{1}{2 \cdot \pi \cdot f_{\text{tuned}}} \right)^2 \quad (2.32)$$

The tuned frequency is calculated as

$$f_{tuned} = \frac{1}{2 \cdot \pi \cdot \sqrt{L_{RLC} \cdot C_{RLC}}} \quad (2.33)$$

### 2.6.3 Converter side filter

One can also place a filter at the inverter side in the configuration. By placing the filter on the inverter side of the configuration the filter could be placed in a less exposed environment like onshore or in a buoy. In order for the generator to operate on the rated torque the inductance should not exceed 0.15p.u [65].

A passive filter designed for the inverter side which is less exposed compared to the generator side can have the opportunity to have different topologies. With different types of connection or grounding the same passive, differential mode filter can affect the common mode voltage as well. The common mode voltage can be reduced by connecting the y-connection of the filter with a DC-voltage, ground or the DC-link of the inverter.

An LCR filter placed at the inverter side with the inductance in series with the transmission cable and the capacitor with the resistance shunt connected increase the derivative of the voltage step [65]. The values of the LCR-filter are calculated, where the resistor  $R_{LCR}$  of the filter is

$$R_{LCR} = \text{real}(Z_C) \quad (2.34)$$

where  $Z_C$  is the impedance of the cable.  $R_{LCR}$  is used to obtain the inductance

$$L_{LCR} = R_{LCR} \cdot \frac{2 \cdot t_{travel} \cdot (\Gamma_{Gen} + 1) \cdot \Gamma_{Gen}}{\Delta V_{max} + 1 + (\Gamma_{Gen} - 1) \cdot (\Gamma_{Gen} + 1)} \quad (2.35)$$

where  $\Delta V_{max}$  is the maximum voltage deviation and  $\Gamma_{Gen}$  is the reflection coefficient at the generator. The capacitance of the LCR-filter,

$$C_{LCR} = \frac{4 \cdot L_{LCR} \cdot \zeta^2}{R_{LCR}^2} \quad (2.36)$$

where  $\zeta$  is the damping ratio of the filter which represent how fast the oscillation is damped and is a value between 0-2, where 0 represent no damping and 2 a major damping of the signal [65].

#### 2.6.3.1 Filter return-connected to DC-link

A common filter that is used in many commercial applications is an inverter LCR filter connected in a y-connection that is left floating. The LCR filter is relatively cheap and simple, however, it does not always give the desired result. This filter mitigates the differential mode  $dV/dt$  to reduce the generator reflection phenomena. By connecting the floating point of the capacitors of the LCR filter back through diodes to the + and -, of the DC-link the common mode voltage can be reduced as well [72]. This topology for the filter requires that the capacitor branch is divided up into two parts with one connected to the  $+V_{dc}/2$  and one to

$-V_{dc}/2$  [15].

Another similar filter topology is having an LCR filter that is connected back to the neutral point of the DC-link, the middle of the capacitors [72].

### **2.6.3.2 LCR Filter grounded**

The y-connection of the filter, the point where the three phases are connected is a common mode point of the system. By grounding this connection the common mode voltage will be reduced through the filter as well as the differential mode filter. The LCR filter is designed in the same way as the other converter side filters with the exception of the connection to ground [4]. The LCR filter is a  $dV/dt$  filter and reduces the risetime of the pulses that passes the filter.

# 3

## Method

In order to understand the task the project started out with a literature study. Scientific literature such as books, articles and papers were read and analyzed. When sufficient knowledge was gathered and the analytic modeling of the system and components took place. The modeling started out with simplified versions of the components and was improved once the system was modeled with all the components together.

### 3.1 Modeling

The analytic modeling started out with a simplified model of the system in LTspice. The generator and the inverter were modeled as a voltage source and additional components in LTspice. The cable was modeled as  $\pi$ -sections. The parameters for the  $\pi$ -section were calculated in Matlab from R,L and C of the cable.

#### 3.1.1 Cable

From the IEEE standard 835 the cable thickness can be selected [44]. By using the current flowing in the cable and the thermal conductivity as a reference one can use the tables from the standard to find an acceptable cable thickness.

Development of the cable model has gone from using  $\pi$ -sections to investigating the frequency content of the system to updating the cable model to be better suited for this project. During simulations for high frequency content for the system it was noted that the previous choice of having 10MHz as the upper frequency boundary for the simulations was necessary.

The case of 2.8kV generator is a very unusual case which means that there are no off the shelf products for that specific case and therefore the cable was chosen as close to the application as possible. The reference cable that was chosen was a 12kV cable. This cable is slightly overdimensioned but gives the cable a longer life span, less water treeing and the cable is available [7].

While modeling the transmission cable there are several models to choose from. In this project the distributed  $\pi$ -model has been chosen because it includes a voltage drop over the transmission line and represents a transmission line in transient simulations well enough to see the phenomenon of reflections that is investigated. The model has been compared to the

### 3. Method

---

theory in transient simulations in LTspice. One can also see the difference that comes with a larger number of  $\pi$ -sections. With an increase in the number of  $\pi$ -sections in the model the range of frequencies that are well represented goes up. From an fast fourier transform FFT of the different numbers of  $\pi$ -sections resonance spikes are clearly visible. The number of those spikes goes up and the frequencies of where they appear goes up as well. Therefore the number of  $\pi$ -sections chosen are such that the interesting frequencies are well represented.

In order to get a good enough model of the cable the equation (2.18) to calculate how many  $\pi$ -sections the model needs have been used. To compliment this an FFT was investigated from the simulaitons in LTspice. There it is possible to see that the resonant frequencies of the cable model.

Losses is another thing that varies with the model being used. The dielectric loss is one of those losses, however, it can be neglected for low voltages [74]. Therefore the dielectric loss has been neglected in this project, conduction losses are represented in the resistive part of the cable model.

**Table 3.1:** Parameters of the chosen 3.3/4.2 kV cable from Nexans

<b>Operating voltage [kV]</b>	12	3.3/4.2	0.6/1
<b>Characteristics</b>			
<b>Design features</b>			
Conductor material	Aluminium	Copper	Copper
Insulation	PEX	Silicone rubber	Polyethylene
<b>Dimension features</b>			
Number of conductors	3	119x0.40	Not known
Conductor area [ $mm^2$ ]	25	16	50
Conductor diameter [ $mm$ ]	5,9	5.55	8.2
Diameter across insulation [ $mm$ ]	13.4	10.35	11
Insulation thickness [ $mm$ ]	3.4		
<b>Electrical characteristics</b>			
Resistance [ $\Omega/m$ ]	1.2	1.240	0.40
Capacitance [ $\mu F/m$ ]	0.2	Calculated	Calculated
Inductance [ $mH/m$ ]	0.39	Calculated	0.24

#### 3.1.1.1 Example of $\pi$ -section of cable

Choosing a cable with known R, L and C parameters and implementing that into the  $\pi$ -model is relatively simple. Using (2.6) to (2.18) the parameters for the  $\pi$ -model can be extracted and implemented into a simulation, in Table 3.2 two examples of 100m and 500m cables are presented for a voltage level of 2.8 kV. The hyperbolic correction is preformed at the frequency  $\omega$  which is the rated rpm of the generator [75].

**Table 3.2:** The table shows two examples of the parameters for the  $\pi$ -model for up to 10MHz for 100m and 500m at a voltage level of 2.8 kV.

Cable length	100 m	500 m
$R_{pi}$	1.926 m $\Omega$	1.937 m $\Omega$
$L_{pi}$	0.542 $\mu$ H	0.545 $\mu$
$C_{pi}$	0.285 nF	0.286 nF
Number of $\pi$ -section	72	358

### 3.1.1.2 Transient model for simulations

When building the model for transient simulations the common practice is to measure the cables impedance and build the model from the results [76]. One method to model a cable that includes high frequency parasitic effects is to measure the cable and then with trial and error find the best match with the simulations [77]. While this method gives the best accuracy this have not been possible in this project.

In this project the cables have been assumed to be individually shielded. This means that the high frequency components will not have connections between the phases but only to ground. The shield losses are neglected and the shield can therefore be considered as ideal.

### 3.1.2 Generator

The selected generator for the project were modeled as common mode model since they had the strongest correlation to the actual configuration of the generator of interest. This generator was not grounded at the neutral of the windings and therefore the common mode was chosen. To model the generator as common mode the circuit consisted of a resistance, an inductance, a capacitance and a back-EMF, the model also include the common mode resistance  $R_m$  and capacitance  $C_m$  as can be seen in Fig. 3.1. For the three phase model the same parameters was used and the model can be seen in Fig. 3.2.

The modeling of the PMSG needs to be accurate for a relatively large frequency spectrum, including high frequencies since transients are in effect on the system. Therefore a multiple section lumped parameter model is suited [61]. This model is accurate for a wide range of frequencies. In the three phase case each of the three phases are identical and consists of three resistances, an inductor and a capacitor in parallel [78], [79]. During the modelling the resistances and the impedances will be approximated to a fixed value. To find these parameters the literature shows that measuring on the generator in every project is needed because of the differences in parasitic parameters in every machine. Since this project does not have that kind of resources instead one can use a simpler model to get a better match with the generator in this project [23].

The resistance  $R_s$  and the inductance  $L_s$  is the resistance and inductance of each stator phase winding of the generator. The stator inductance  $L_s$  is an average value of  $L_d$  and  $L_q$  which depends on how the generator is built. If the generator is salient  $L_d$  and  $L_q$  are equal and if it is non-salient  $L_d$  and  $L_q$  are different. The capacitance  $C_s$  is the parasitic capacitance

### 3. Method

between the turns of the winding in each phase. The parasitic capacitance was chosen to  $1.1nF$  for both the  $400\text{ V}$  and  $2800\text{ V}$  generators since it could not be determined for the specific generators since there were no generators to measure on.

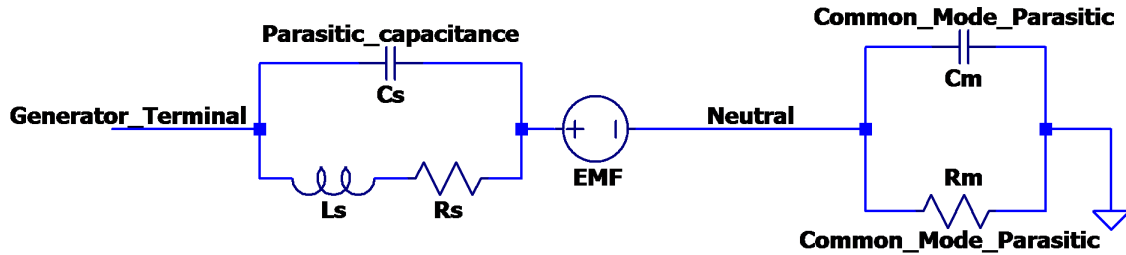


Figure 3.1: The circuit diagram of the generator for one phase

Between the windings and motor frame there is a space which is insulated, the space is modeled with a parasitic capacitance  $C_m$  and a resistance  $R_m$  in parallel. The value of parasitic capacitance  $C_s$  and  $C_m$  are based from the literature and the resistance  $R_m$  is chosen as a similar value, these and all the parameters for the generator can be seen in Table 3.3 [14].

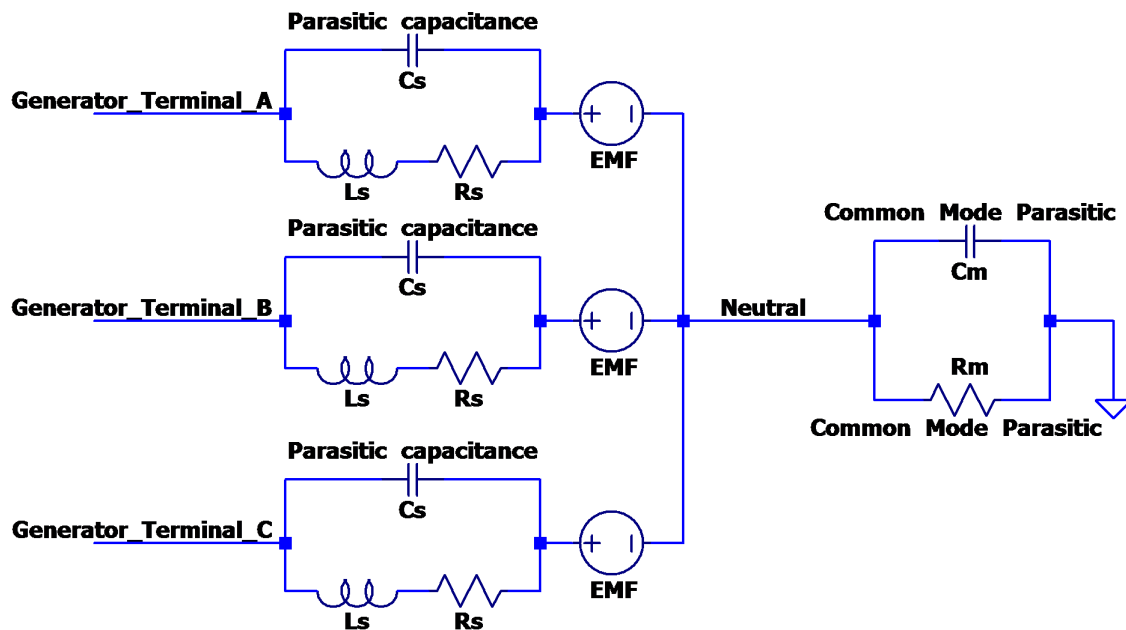


Figure 3.2: The circuit diagram for all three phases of the generator

**Table 3.3:** Parameters of the two different generators, 400V and 2.8kV

Nominal line voltage [ $kV$ ]	2.8	0.4
Generator type	PMSG	PMSG
Number of poles	12	4
Nominal S [ $kVA$ ]	60	60
Nominal P [ $kW$ ]	52.28	50
Nominal speed [ $rpm$ ]	4000	1500
Nominal torque [ $Nm$ ]	119.4	319
No load EMF line-to-line rms [ $kV$ ]	2.28	0.425
Stator resistance $R_s$ [ $\Omega$ ]	1.3235	0.005
Stator inductance $L_d$ [ $mH$ ]	12.91	0.112
Stator inductance $L_q$ [ $mH$ ]	35.82	0.112
Stator inductance $L_s$ [ $mH$ ]	24.36	0.112
<b>Chosen parameters for model</b>		
Parasitic capacitance $C_s$ [ $nF$ ]	1.1	1.1
Common mode parasitic $C_m$ [ $nF$ ]	7.7	7.7
Common mode parasitic $R_m$ [ $\Omega$ ]	$1e^6$	$1e^6$

The high frequency components are usually obtained by measurements on a suitable generator, this was unfortunately not possible during this Master's Thesis. This is preferable since major part of the high frequency components depends on how the generator is built, size, dimensions, windings and the insulation. A more accurate procedure to obtain the parameters of the generator would have been to use an RLC meter to measure on a specific generator and see how the generator would behave in the frequency spectra of interest and then apply that to the model. This would have increased the accuracy of the simulations and the results.

### 3.1.3 Inverter model

In order to obtain a realistic model of the inverter, the PWM signal from the inverter was in focus in the project. This, since the inverter have several parameters that strongly affects the overvoltages at the generator. Therefore changing these parameters in the system have been one of the main focuses. This in order to obtain understanding of correlations between the overvoltage and the inverter parameters.

There are in power electronics a few different technologies for controlling the switches. Depending on what voltage and power levels needed some of these types of switches are better suited. In a power production application with the voltage and power level such as in this project the IGBT technology is the industry standard. For the selection of the IGBT, investigations in the literature has been performed as well as searching for available products on the market. The chosen inverter was selected from an available product from Infineon and the chosen IGBT was a switch which had a rated voltage of 1700V and 100A [80]. The rated risetime of the chosen IGBT is  $50ns$ , this risetime is only valid in laboratory environments and therefore this fast risetime is not used.

For IGBTs the risetimes are usually around 10ths of  $ns$  therefore are there simulation with

risetimes down to  $10ns$  in the project [8]. The risetime was in the earlier parts of the study swept over a large range, larger than any reasonable risetime for a state-of-the-art inverter, and also faster than an inverter for this specification would be. This to see how the risetime affects the voltage of the system. Depending on the specifications and the material of the switches the risetime can be near  $50kV/\mu s$ . Therefore a more realistic case were simulated with a  $dv/dt$  of  $50kV/\mu s$ , which means that the risetime of the switch have a risetime of  $100ns$  for a DC-link voltage of  $5kV$  [81]. These specifications for the IGBT were further on used in the project for the three phase, multilevel and filter simulations and are concluded in Tab. 3.4.

**Table 3.4:** The table shows the specifications of the chosen IGBT switch.

IGBT switch	
Voltage	1700 V
Current	100 A
Risetime	100 ns

Another part of the inverter model to be selected was the topology. To be able to investigate the impact the topology have on the generator voltage, three different topologies were interesting, 2-level, 3-level and 5-level inverters. To get an understanding of how the magnitude of the voltage affected the overvoltage the 2-level inverter was first to be implemented and the topology can be seen in Fig. 3.3. In the 2 level inverter the voltage applied over each switch is  $V_{DC}$ , this creates a very high voltage over each switch. The switch therefore consists of several switches in series where the number of switches are calculated by

$$\text{Number of switches} = \frac{\text{Applied voltage} + 20\%}{\text{Rated voltage of switch}} \quad (3.1)$$

where the number of switches connected in series for this case is four to withstand the voltage (3.1). This due to the DC-link voltage is  $5000V$  and the rated voltage of the switch is  $1700V$ . This set up can also be seen in Fig. 3.3 of the 2 level inverter. These switches are assumed to switch simultaneously and therefore the rated risetime of the chosen IGBT will apply and create a pulse that have a  $dv/dt$  of  $50kV/\mu s$ .

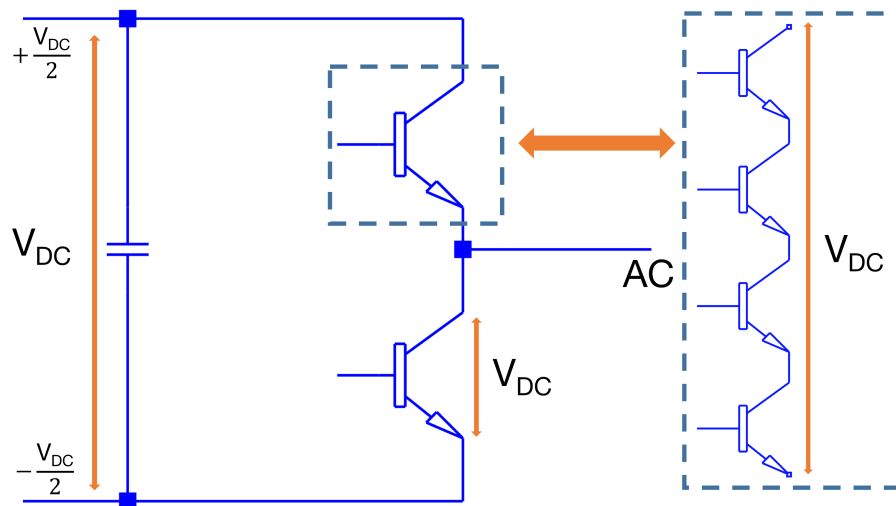


**Figure 3.3:** Inverter topology for the 2 level switch, where each switch consist of 4 switches to be able to handle the voltage level over the switch. The three switches are assumed to switch simultaneously.

When applying the 3 level topology the voltage applied over the switch is lower. Since the voltage over the switch is lower, the number of switches to withstand the the voltage is two, this can be seen in Fig. 3.4. These switches also switch simultaneously and therefore the rated risetime of the switch create a lower  $dv/dt$  of the pulse since the applied voltage is lower. This means that when the lower voltage is applied over the two switches the  $dv/dt$  of the pulse become lower than the for the 2-level topology, this can be seen in Fig. 3.6.

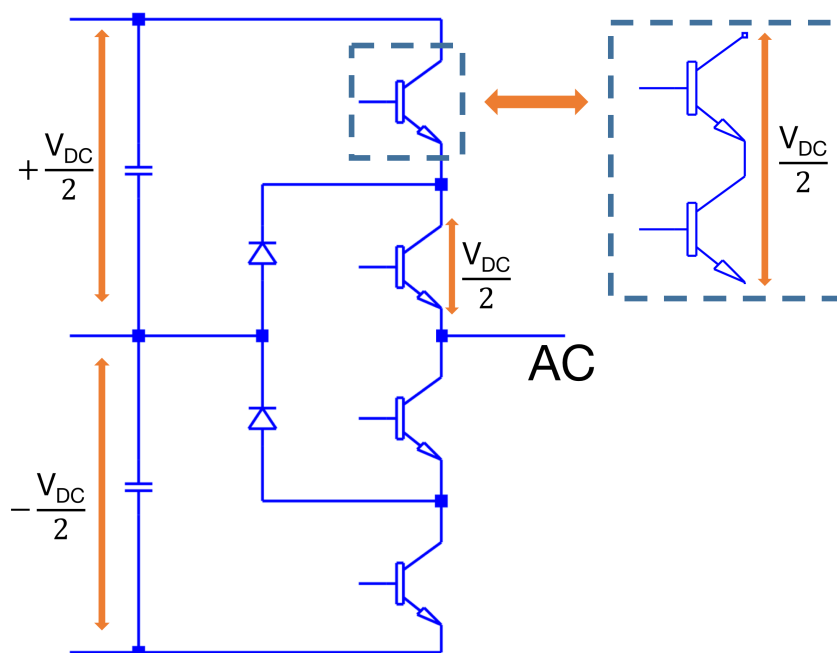


**Figure 3.4:** The figure shows the inverter topology for the 3 level inverter. Each switch in this case consist of two switches to be able to handle the voltage over the switch.

### 3. Method

When the number of levels are increased further to 5-level, the voltage applied over the switch become even lower. From the same principle as in the 3-level case the  $dv/dt$  decrease even more. This configuration is more complicated to control due to the large number of switches.

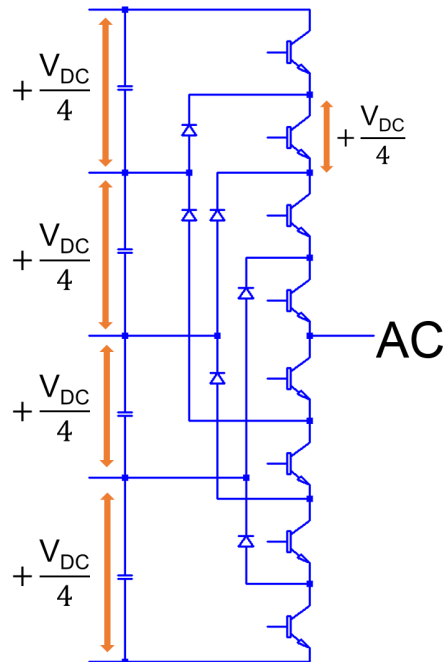


**Figure 3.5:** The figure shows the inverter topology for the 5 level inverter. Where the voltage over each switch is low enough to be handled by one switch. The 5 level inverter reduce the amplitude of the pulses and thereby the  $dv/dt$  of the voltage.

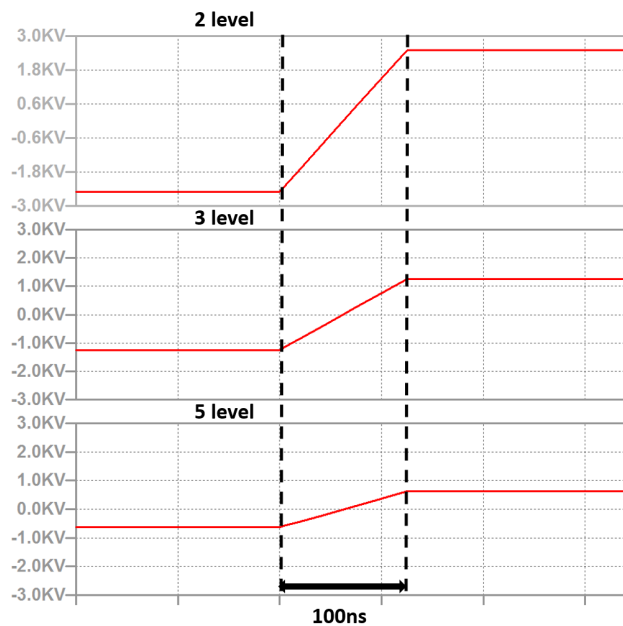


**Figure 3.6:** The figure shows how the risetime is kept constant for each level of the inverters while the applied voltage is reduced and thereby lower the  $dv/dt$  of the pulse.

From the parameters of the inverters in a reflection coefficient calculation it can be noticed that the low values will result in a very low reflection coefficient, approximately -1. This is because the switches can be seen as stiff in this scenario. The switches have low parasitic parameters and in the model of the cable the cable parameters are significantly higher, resulting in that the small values of the inverter can be neglected.

### 3.1.4 PWM generation

When the reference wave is larger than the carry wave the output of the converter legs should be positive. When the reference is smaller than the carry wave the output of the converter legs are negative [38].

The inverter that has been used is a bipolar inverter with IGBT switches that are controlled to switch a PWM pattern to control the generator. To model the switching the inverter has been kept to the simplest model possible, the waveforms are generated in Matlab with a specific risetime and switching frequency and exported as a .txt-file. The .txt-file was then imported into LTspice to a voltage source and sent on to the cable. The switching used in this project has been implemented without zero sequence injection.

The PWM signal for the simulations is generated in Matlab and has been created by comparing a carrier waveform as a sawtooth waveform with a set switching frequency to a sinusoidal waveform with a frequency of 50 Hz as the reference. The frequency of the sawtooth waveform and therefore also the switching frequency was 8 kHz because this is a value that is close to what commercial inverters use today. The switching frequency from 500 Hz to 5000 Hz have also been studied to achieve knowledge and show the relationship between overvoltage and the switching frequency.

The voltage amplitude is chosen depending on which system is being simulated. For the low voltage case the max voltage is  $+400 V_{DC}$  and the min voltage is  $-400 V_{DC}$ . For the case with a voltage of  $2800 V_{RMS}$  the voltage at the DC-link was set to  $+2500 V_{DC}$  and  $-2500 V_{DC}$ . This represent the DC-link voltage of which the inverter switches. The DC-voltage has a high enough voltage to have a buffer in the voltage for the amplitude modulation  $m_a$  to be set to a lower value than 1.

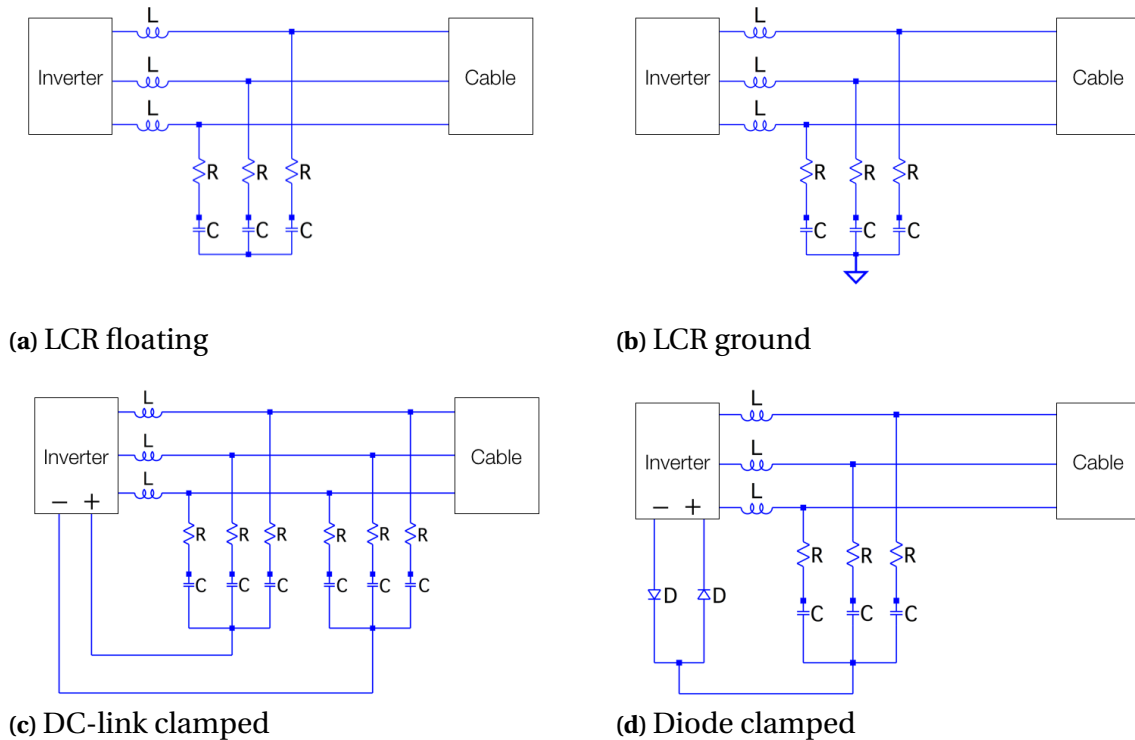
### 3.1.5 The filters

The filters treated and simulated have been the ones that were found in the literature to have the lowest losses and the best overvoltage mitigation in comparable systems. Since the cable model was assumed to have the phase conductors separately shielded the use of components such as mutual inductance transformer have not been used.

Because of the background and the concept of the Deepgreen technology which was the intended target for the study the most interesting filter was one where it is located at the inverter side. The filter that through literature study was found to be the most effective to compensate differential mode voltages was the LCR filter at the inverter side, therefore the study is made on this filter [4], [11]. Different filter topologies that have shown the most

### 3. Method

interesting solutions have been tested and compared in simulations, the schematics of the different filter configuration can be seen in Fig. 3.7.

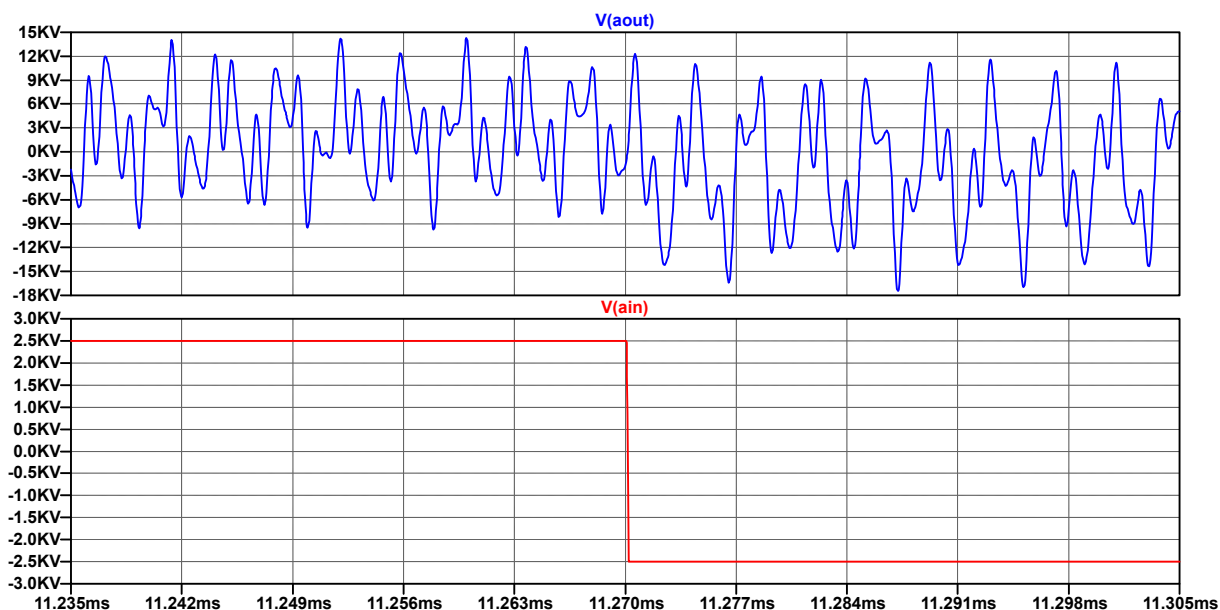
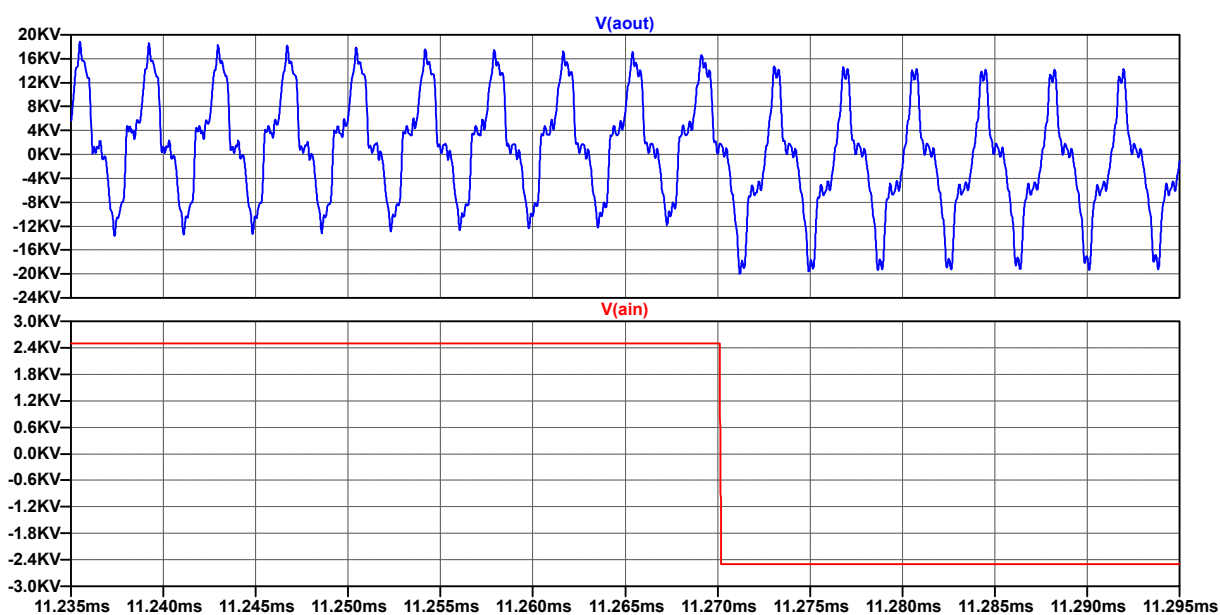


**Figure 3.7:** Filter topologies for inverter side LCR filter

## 3.2 Simulations

The simulations in this project were performed using the program LTspice with a transient analysis mode. LTspice is a relatively simple program for the types of simulations used in this project. It does however require quite much to run the simulations such as computing power, hard drive storage and time. Since the interesting point of the project is overvoltages and high frequency content in form of harmonics and reflections the transient analysis tool that LTspice can produce is suited to be the simulation software [82].

The number of  $\pi$ -sections that the cable is modeled with is important, as the theory suggest. In Fig. 3.8 this can be seen. By building 100  $\pi$ -sections and distributing the parameter values, the resulting waveform at the generator terminal changes drastically. Even though the rest of the simulation is exactly the same the overvoltages at the generator terminal is about one third with the 100  $\pi$ -section simulation compared to the 4  $\pi$ -section simulation. This happens because with more  $\pi$ -sections higher frequencies are more accurately shown. In Fig. 3.8 the difference of the two cases can be seen. When the high frequencies are represented the simulation becomes more accurate. The addition of the voltages is present in both cases, but when the high frequencies are well represented they add together to form a more accurate representation of the voltage.

(a) 4  $\pi$ -sections(b) 72  $\pi$ -sections

**Figure 3.8:** 4  $\pi$ -sections vs 100  $\pi$ -sections zoomed in on one switch. It can be seen that the simulation with 72  $\pi$ -sections have a higher bandwidth and will therefore be more accurate.

### 3.2.1 Simulation circuits

In order to get the simulations comprehensible the first simulations were simplified one phase models with a bipolar PWM inverter switching method. The voltage of the system were phase voltage to ground. The DC-link voltage or the voltages of the hypothetical inverter before the simulation is considered in this first case to be  $+DC/2$  and  $-DC/2$ , more specifically in the lower voltage case  $+400V_{DC}$  and  $-400V_{DC}$ . In the medium voltage case the line-to-line voltage was considered to be  $2800V_{RMS}$ . That correlates to  $+2500V_{DC}$  and

### 3. Method

-2500V<sub>DC</sub> on the DC link of the inverter. In the three phase case the same system was used in order to keep the results as close to the different cases as possible. In the three phase case the phase voltages have the same exact waveform with the exception of being 120deg phase shifted to each other.

In a three phase transmission system the cables are in close proximity of each other and will interact with each other, this is called mutual characteristics. The inductance and the capacitance affects each other and change the characteristics of the cable. However, if the conductors are screened and grounded individually or have a sufficient distance from each other the mutual impedance will be very small or negligible. Since the phases are screened the mutual impedances between the conductors have been assumed to be negligible. The cables have a capacitive connection to ground and a self inductance as parasitic component.

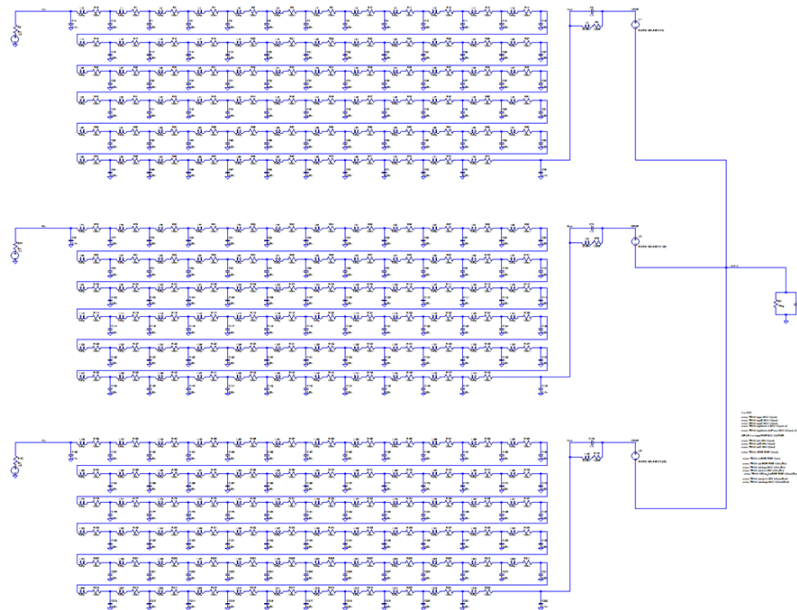


**Figure 3.9:** Schematic of the three phase system from the Simulation.

Therefore is the 3-phase model an extension of the one phase model. For the three phase system the model was the same as the one phase system. Since the three phases are identical the one phase model was extended to be three separate ones connected in a y-connection behind the generator windings and the emf, as can be seen in Fig. 3.9. The generator is assumed to be built as common mode connected. That is the reason for the common mode parameters between the neutral point and ground. The parameters are strongly dependent on the geometry of the generator and have therefore been chosen to be example values that were found in literature [14].

### 3.3 Validation of model through simulations

The cable model that is used in this project can be used for various situations. It is well suited for projects with a frequency range up to 10MHz. The more  $\pi$ -sections there are in the model the higher the frequency content it can handle. While performing the simulations the model that have been used is proportional dependent on the length of the cable.

In order to get a 3 phase simulation with high accuracy the 500m model was used and extended to three phases, connected to the generator in y-connection. The cable model is constructed in the same way for different cables but the values depends on the the parameters of the cable. However, when including the mutual impedances, the time and size of the simulation becomes too large for the hard drive which results in a limitation in the projects scope.

#### 3.3.1 Bandwidth

Bandwidth is depending on the risetime. This also correlates on how many  $\pi$ -sections that is used. With a faster risetime there is an estimate proportional increase in the frequency content as well. Therefore the expected range of the frequency content for a switch with a risetime of 10s of nanoseconds would be about 10MHz can as a rule of thumb be calculated from (3.2). Therefore an accuracy of up to 10MHz for the cable model was implemented and verified through FFTs

$$\text{Bandwidth [Hz]} = \frac{0.35}{\text{risetime [s]}}. \quad (3.2)$$

#### 3.3.2 Wave propagation

When the PWM waves are sent through the cable the waves are reflected at the generator side, travel back on the cable and then reflected back again at the inverter. The speed of the travelling wave through the cable depends on the material which the cable made of. The velocity was calculated according to (2.22) for the two cables that was used in the project, the 3.3/4.2 kV cable, which is shown in Table 3.5.

**Table 3.5:** The table shows the velocity of the wave in the cable and the calculated and simulated time it takes for the wave to travel over the cable.

Cable type	Velocity [km/s]	Calculated time [ $\mu$ s]	Simulated time [ $\mu$ s]
2800V XLPE	1.12e5	0.894	0.894

To show that the calculated time match the simulated time for the propagating wave, measurements of the time were made in the graphs from the simulations. From Fig. 3.10 it can be seen that when the PWM switch from positive to negative the generator terminal respond after 0.89  $\mu$ s, this is approximately the same time it takes for the wave to propagate over the cable which was calculated for the 2.8kV cable. This means that when the the inverter switch the wave start to propagate over the cable and reach the generator terminal after 0.89  $\mu$ s.

### 3. Method

The wave is there reflected back to the inverter and at the inverter back again to the generator terminal. This is why the voltage increase again after  $3.58 \mu s$  which is  $2x$  the time it takes for the wave to travel back and forth over the cable which can be seen in Fig. 3.10.

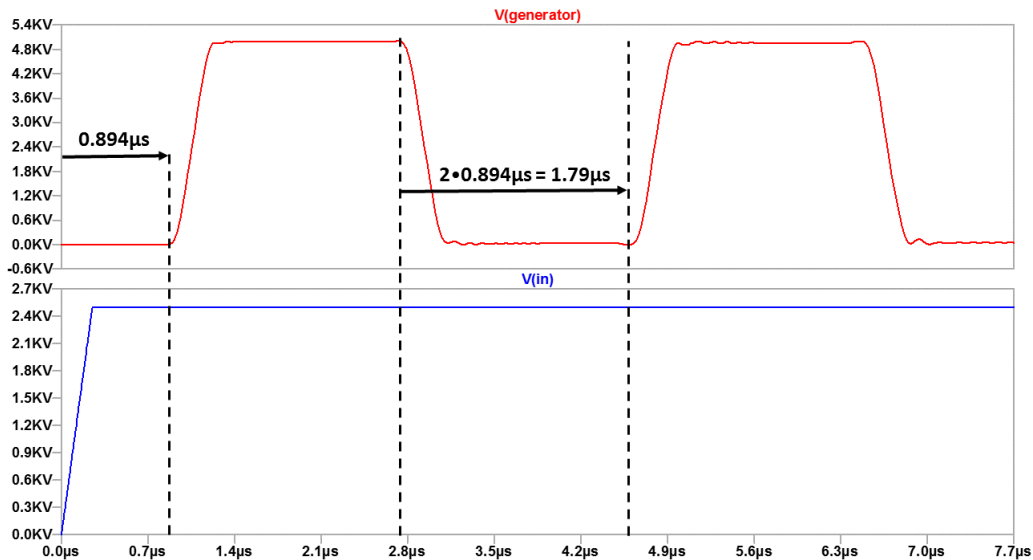


**Figure 3.10:** Reflection of one pulse being sent towards the generator over a long transmission cable rated for 3.3/4.2 kV. The figure shows the time it takes for the wave to reach the other side of the cable and the time it takes for the wave to be reflected propagate back and forth and return to the generator.

#### 3.3.3 Accuracy of LTspice

When simulating with LTspice there are a few criteria that needs to be fulfilled to get the desired result that can be analyzed. One of these is the sampling time of the simulation. If the sampling time is too long the results of the simulation will not include the high frequency components that are interesting here. By either setting the sampling time in LTspice or having a thorough input waveform this has be achieved.

When using LTspice for simulations it is important to know that there are limitations to the software. Since the simulations for this project investigates high frequency content there is a high demand on the sampling time. One thing to do to increase to accuracy of the LTspice simulations is to increase the number of time steps used in the simulation. By increasing the number of timesteps in the PWM the accuracy of the simulation increase. With this increase in accuracy the time that is required to perform the simulations increase as well.

In the simulations the voltage at the inverters three phases are set as definite voltages. The voltage source in LTspice creates the voltage and sets the voltage to the value given. Since the voltage source is grounded in one end the voltage in the other will be what the voltage source is set to and will not be affected by the rest of the system. That is why the voltage at the inverter is ideal.

# 4

## Results

In this chapter the results from the study are presented and analyzed. First the systems characteristics and behaviours are presented and then a realistic case is used for reference and overvoltage mitigation through filtering.

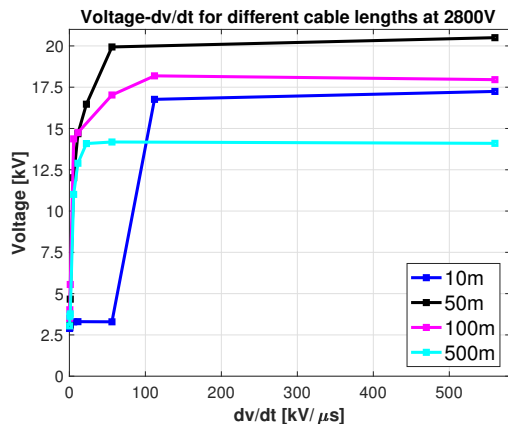
### 4.1 Overvoltage dependency

In LTspice the effect of the risetime of the PWM pulse, the length of the cable and the switching frequency were investigated to see how the voltage at the generator behaved when sweeping the three parameters. These tests were done with a one phase model connected to a common mode modeled generator.

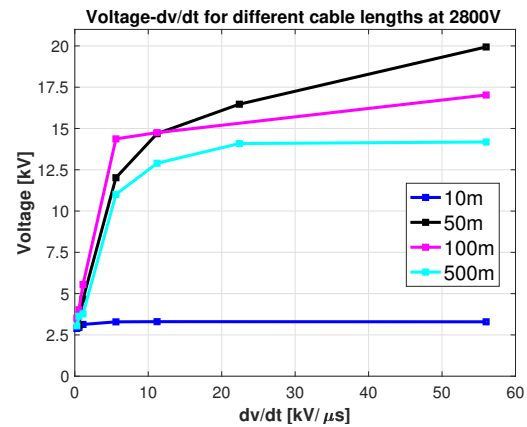
#### 4.1.1 Risetime and cable length

The setup in these simulations was a single phase model where the the number of  $\pi$ -sections is determined according to (2.18) for each length for each case and to have the 10MHz frequency range. The parameter values used for the cable and generator can be found in Tables 3.1 and 3.3. The generator is seen as being in no-load mode and the EMF has zero phase shift compared to the respective PWM signal from the inverter. The voltage on the generator terminal for one phase is presented with the risetime of the PWM pulses of the inverter signal. The simulations have been performed with different risetimes, the maximum absolute value of the voltage of the simulations have been plotted together with its respective risetime. It can be seen in Fig. 4.1 and Fig. 4.2 that the characteristics of 2800 V and 400 V are about the same for the parameter that is swept. The voltage has, as can be seen in Fig 4.1(b) a fast rise in the overvoltage when reflections start to occur. The effect will saturate when the reisetime has become fast enough for the system, which can be seen in Fig 4.1(a).

## 4. Results

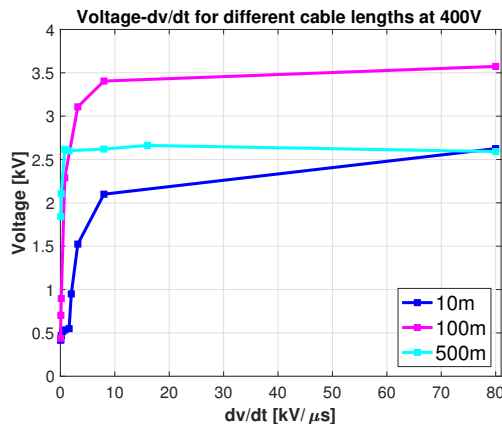


(a) Generator terminal voltage to ground compared to inverter risetime with 2800V DC-link voltage.

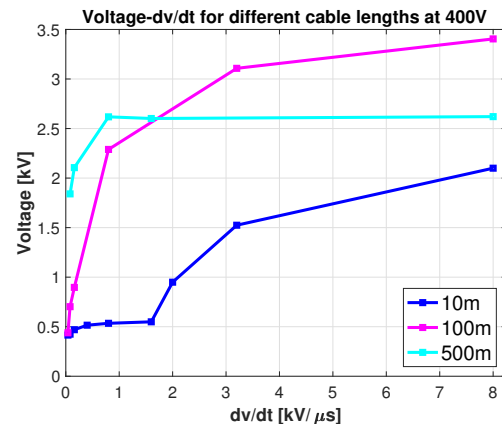


(b) A zoomed part of the lower dv/dt in (a)

**Figure 4.1:** In Figure (a) voltage dependency on dv/dt is shown and in (b) a zoomed part of the graph is shown.



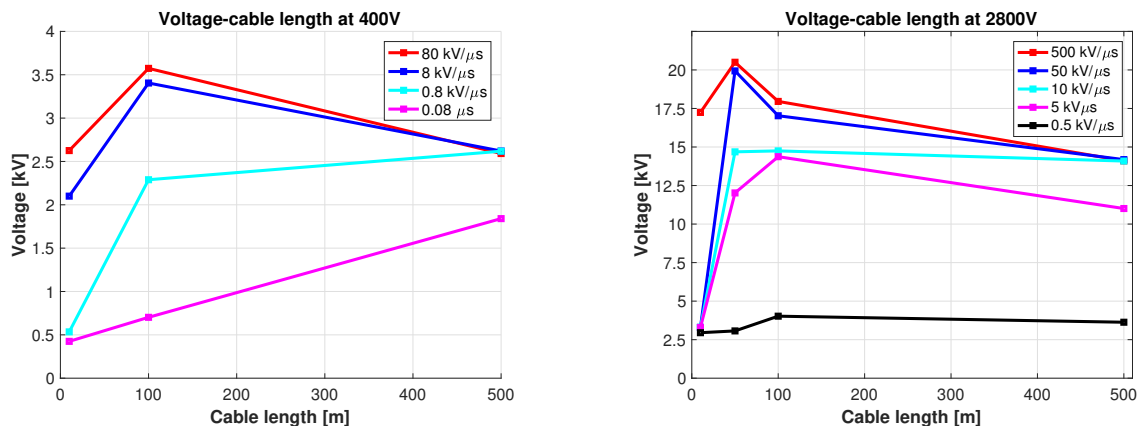
(a) Generator terminal voltage to ground compared to inverter risetime with 400V DC-link voltage.



(b) A zoomed part of the lower dv/dt in (a)

**Figure 4.2:** In (a) voltage dependency on dv/dt is shown and in Figure (b) a zoomed part of the graph is shown.

From Fig. 4.3 it can be seen that the voltage at the generator terminal is increasing at first with an increasing length of the cable but when the cable become longer the voltage decrease instead. This depends on the increasing impedance of the cable and therefore more damping, since the cable gets longer the total impedance of the cable is increased, which also means that the reflection coefficient from (2.19) will decrease. The decreased reflection coefficient results in on lower overvoltages on the generator terminal.



(a) Generator terminal phase voltage compared to the length of the transmission cable, voltage input of the DC-link is 400V.

(b) Generator terminal phase voltage compared to the length of the transmission cable, voltage input of the DC-link is 2800V.

**Figure 4.3:** Voltage depending on cable length is shown for 400V (a) and 2800V in (b).

From the results of the simulations the correlation between the length of the transmission line and the  $dv/dt$  of the PWM pulse can be seen. If the system has a longer cable the overvoltage becomes significant for  $dv/dt$  that are larger than for the short cables. This correlates with the theory. By using a longer transmission cable or a faster  $dv/dt$  the overvoltage at the generator terminal is expected to be more problematic.

#### 4.1.2 Frequency dependency

The switching frequency is another parameter that can cause the voltage to increase, when the voltage pulses occur shortly after each other. Before the first pulse has time to get damped down the new one adds its voltage to the existing and the total voltage is increased, this can be seen in Fig. 4.4. When short pulses do not have time enough to be damped in amplitude because of a high reflection coefficient the next pulse will have its amplitude added to the already existing voltage on the transmission line. This phenomenon has most impact where PWM has the highest and lowest duty cycles. When one long positive pulse is followed by one fast negative, or vice versa.

## 4. Results

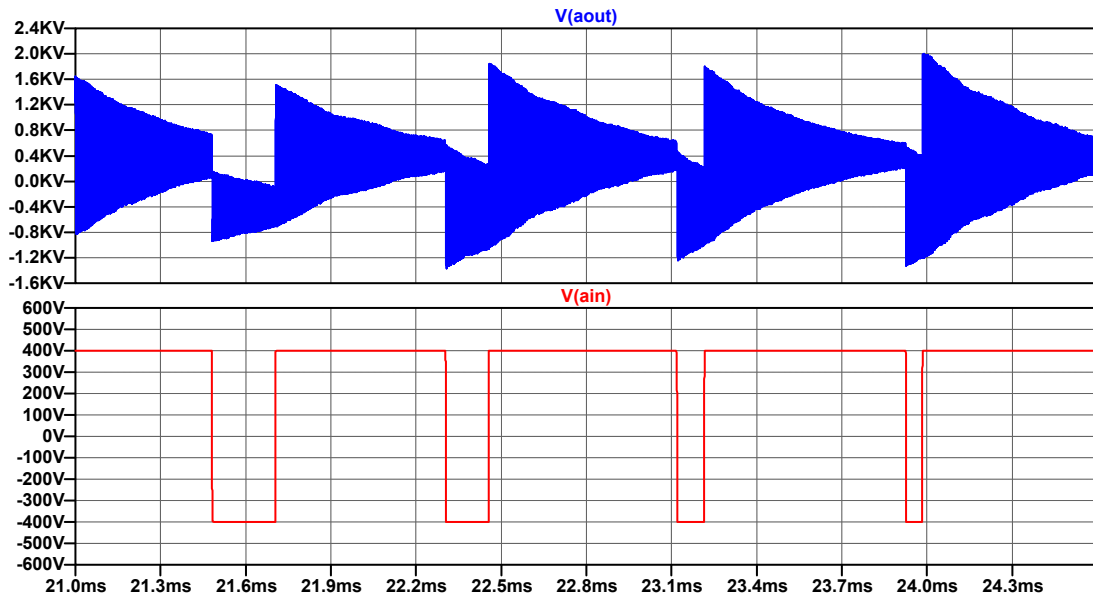


**Figure 4.4:** Voltage pulses interfering with each other and thereby creating a higher voltage. The red curve is the PWM of the input voltage with a decreasing space of the negative part of the pulse. The blue curve is the voltage at the generator terminal which is increased when the pulses becomes shorter.

With an increase in frequency the overvoltage becomes more significant, this can be seen in Fig 4.5 which shows the relationship of the frequency and voltage at the generator terminal. This concur with the theory described earlier. In the case of the system having very fast damping the overvoltages might not overlap at all, resulting in the same overvoltage at every switch.

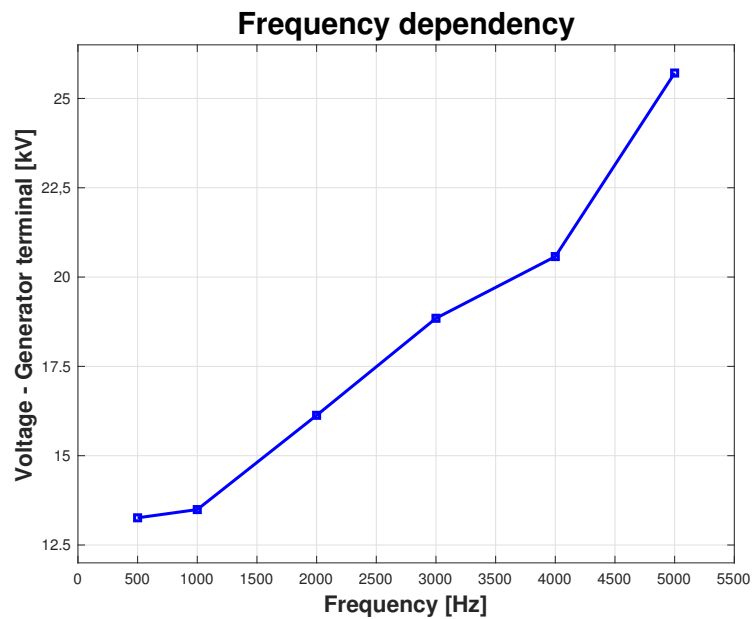
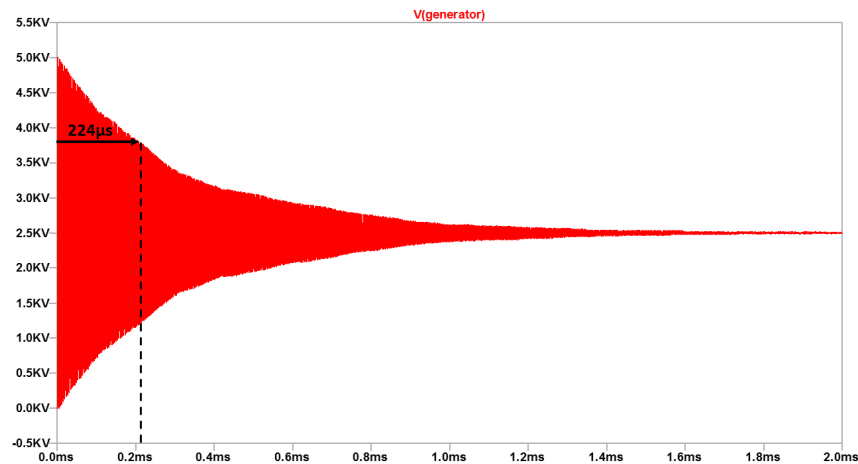


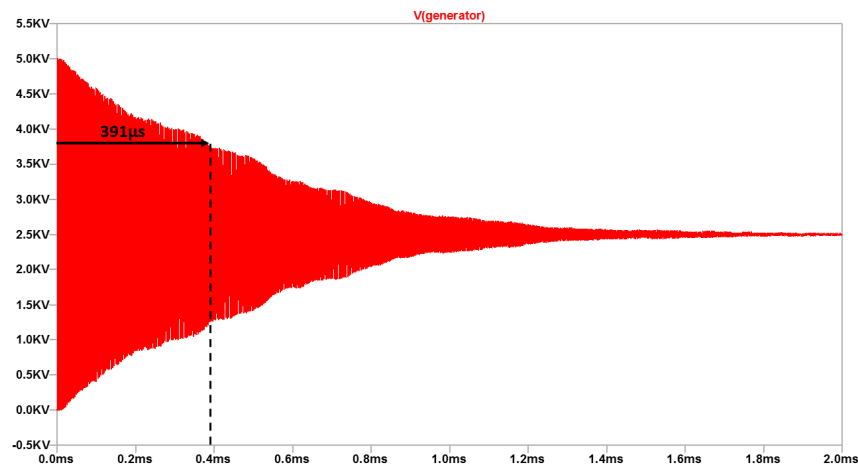
**Figure 4.5:** Voltage compared to the switching frequency, which shows that the voltage increase almost linear to the increasing frequency.

### 4.1.3 Damping of the overvoltage

A faster risetime means that the damping of the overvoltage through reflections takes more time, as Fig 4.6 shows. An increase in time required for the voltage to return to normal is problematic. The longer time the insulation is exposed to overvoltages the earlier the insulation is worn out. Another part is the possibility for wave interference. This means that the magnitude of two, or more electromagnetic waves overlap and the voltage can become very high.



(a) For  $1.5 \text{ kV}/\mu\text{s}$  the time it takes for the voltage to be damped to 50 % of the reflected voltage is  $224 \mu\text{s}$ .



(b) For  $10 \text{ kV}/\mu\text{s}$  the time for the voltage to be damped to 50 % of the reflected voltage is  $391 \mu\text{s}$ .

**Figure 4.6:** The figures show the voltage at the generator terminal due to reflections. It can be seen that if the  $dv/dt$  is larger it also takes longer time for the reflections to be damped.

## 4.2 Multilevel PWM for 1-phase simulations

It was investigated how the number of voltage levels in the PWM affected the voltage at the generator. The voltage was drastically reduced by the increase in number of levels in the PWM. In Table 4.1 the maximum voltage in the different levels can be observed. The maximum value of the voltage is shown as an absolute value. The 1-phase situation was used as a reference case to see what the worst case scenario looks like. The risetime was chosen from a datasheet of an available IGBT product [80] and therefore the  $dv/dt$  is high.

The cable is 100m long and the model has the upper limit on the frequency of 10MHz, which results in a cable model of 72  $\pi$ -section from (2.18). The generator model is the one from Fig. 3.1 with parameters for the 2.8kV from Table 3.3.  $500 \text{ kV}/\mu\text{s}$  is the result of an ideal case with risetimes from a lab environment for an IGBT module together with the desired voltage level for the system and the assumption that is described by Fig. 3.6 [80].

**Table 4.1:** Difference in voltage between 2, 3 and 5 level PWM on a 1 phase system with a cable length of 100m.

Number of voltage levels	Maximum phase voltage [kV]	$dV/dt$ [ $\frac{kV}{\mu s}$ ]
2 level	31.8	500
3 level	18.6	250
5 level	10.3	125

The multilevel converter topology reduces the overvoltage, as expected. The result shows that the theory holds and that a multilevel converter will by itself reduce the overvoltages. The voltages at the generator terminals are still too high and can not be seen as successful. The voltage overshoot is too large for the components to withstand and would result in a reduced lifetime.

## 4.3 3-phase simulations

In the 3-phase model the one phase model has been the base of the structure. The simulations show, Table 4.1, that the phases behave in a similar way in three phase and in one phase. The notable difference in three and one phase cases is the possibility to analyze the line to line voltage. Since the power plant does not have an easy connection to ground or neutral the simplest way of dealing with and analyze the system is through the line to line voltage. This is also the most destructive, because it is higher than any other voltage reference.

**Table 4.2:** Difference in voltage between 2, 3 and 5 level PWM on a 3 phase system rated for 2800  $V_{RMS}$  with a cable length of 100m and 72  $\pi$ -sections.

Number of voltage levels	Maximum phase voltage [kV]	Maximum line to line voltage [kV]	dV/dt [ $\frac{kV}{\mu s}$ ]
2 level	35.27	50.81	500
3 level	18.98	21.35	250
5 level	10.05	14.22	125

For the three phase cases the voltage levels are similar in the phase to ground voltage compared to the one phase cases. The line to line voltage on the other hand is too large. This is due to the fact that phase a and phase b has overvoltages with opposite polarities at some instances and thereby the voltage can become increased when measuring between the phases. A voltage with this magnitude for a system designed for 2800  $V_{RMS}$  would most likely break down or have a severe reduction in expected lifetime. The case is a worst case scenario with ideal components which is why the result are not limited.

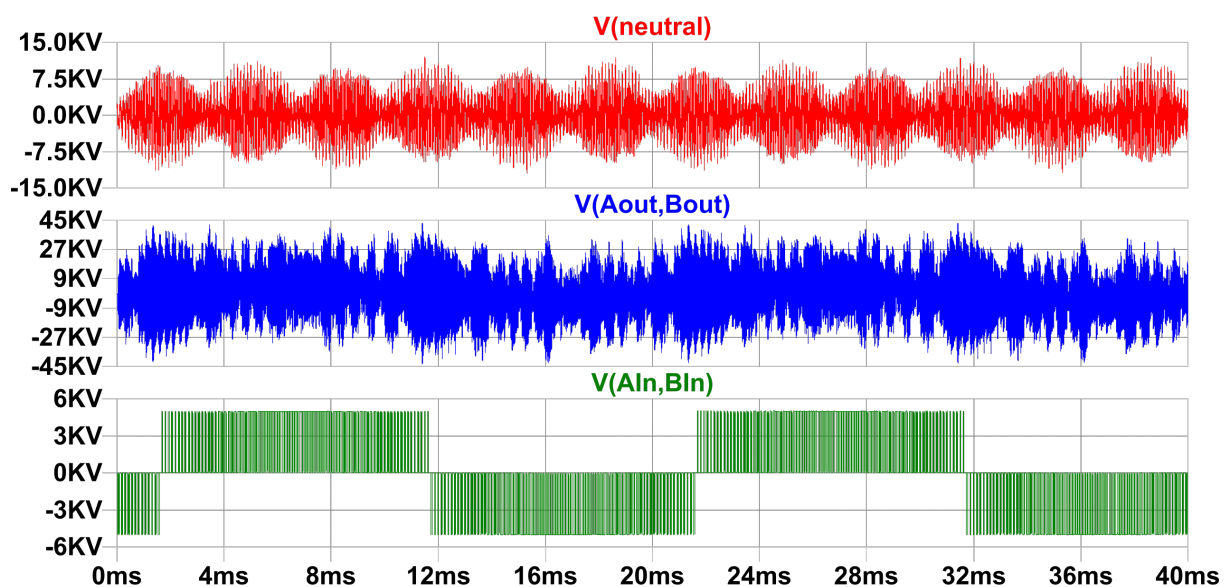


**Figure 4.7:** 3-phase simulation for 2-level PWM.

The waveforms are quite distorted as can be seen in Fig. 4.7 due to the reflections being present, as described in the theory. The neutral point of the generator does not have zero voltage. This voltage is the common mode voltage and changes significantly in a 3-phase system that does not have balanced sinusoidal voltages, as described by (2.3). The high voltages that are shown in Fig. 4.7 needs to be mitigated.

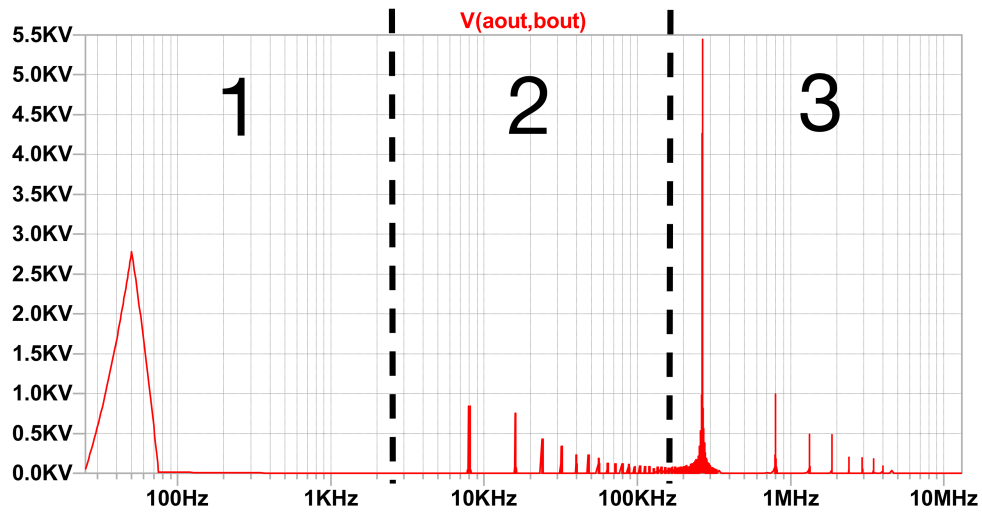
### 4.3.1 FFT analysis

The different frequency components that exist in the system can be analyzed with an FFT. The FFT shows the magnitude of each frequency that is present in the system. The frequencies with high energy content in this system show a high magnitude in the plot. The frequency with the highest magnitude should be the fundamental frequency, which can be found in zone 1 in Fig 4.8. Depending on how much disturbances there is in the system the more peaks there are at other frequencies than the fundamental. The PWM signal has a switching frequency that can be seen in Fig. 4.8 in zone 2, as the first peak after the fundamental frequency. After the switching frequency there are several smaller peaks. These are multiples of the switching frequency and has a lower magnitude at the higher frequencies. In Fig 4.8 zone 2, these harmonics are the last of the high frequency components in the voltage. In comparison, Fig 4.8 shows all the frequencies that the entire system has. In zone 3, the reflection frequency is present which is the frequency that comes from the reflected pulses traveling back and forth on the cable. This frequency needs to be filtered in order to mitigate the overvoltage. The reflection frequency can be described by (2.26) which means that the time it takes for a pulse to travel across the transmission line back and forth will result in a high frequency component in the system. This frequency 270kHz can be seen in Fig 4.8 in zone 3.

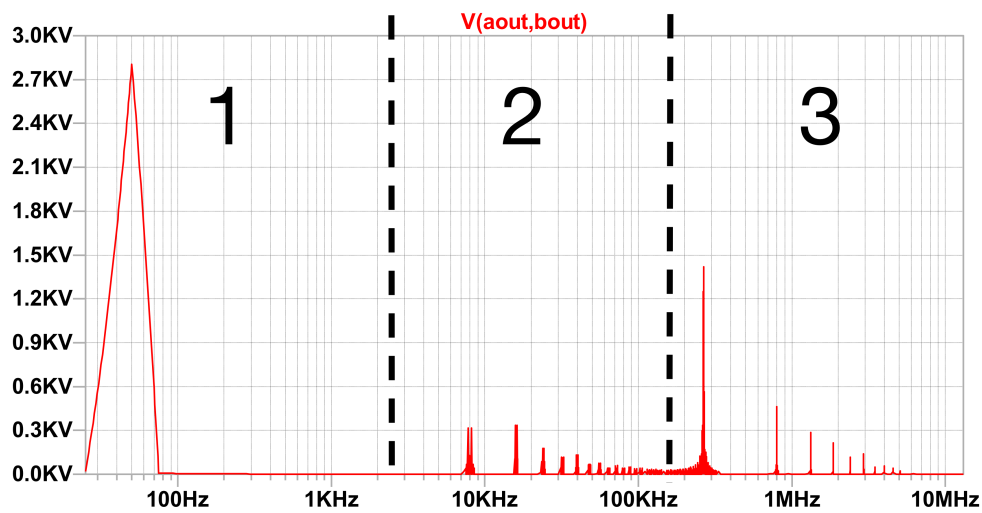
The difference between 2- 3- and 5-level PWM can also be seen in Fig 4.8. For the 5-level case 4.8(c) one can see that components around 8kHz is smaller than for the 2-level case, 4.8(a). This is due to the waveform being closer to the 50Hz sine that is the target.

From this it is possible to see what frequencies there are that needs to be filtered out. The reason that the magnitude spike is wide around the fundamental frequency of 50Hz and not thinner is because the simulation time has to be short because the computer runs out of space. If the simulation time were longer the spike at 50 Hz would just show 50 Hz and not anything around the frequencies close it. The switching frequency of 8kHz for three phases system reduced to 0 in the line-to-line voltage because of the symmetry of the three phases switching.

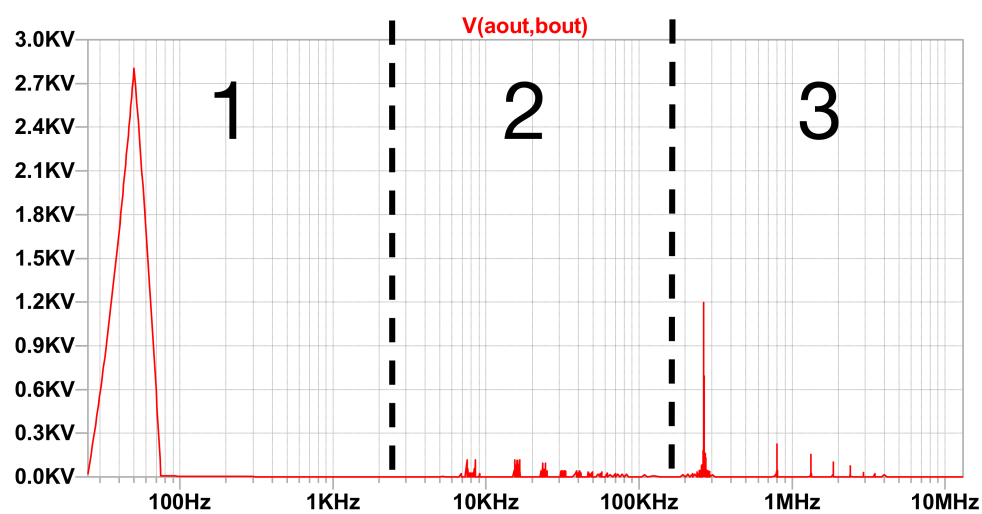
All the frequencies except for the fundamental gives rise to overvoltages. The reason there is overvoltages in the system is due to the fact that there are several voltages with relatively high magnitudes present. When voltages interact with each other they get layered on top of each other. If the different voltages pulses have a peak at the same time the voltage will superpose, the combined voltage at that given time has the highest voltage that the system experiences.



(a) FFT of the line to line voltage of the 3 phase with a 2 level inverter



(b) FFT of the line to line voltage of the 3 phase with a 3 level inverter



(c) FFT of the line to line voltage of the 3 phase with a 5 level inverter

**Figure 4.8:** FFT for the 3 phase cases with  $500kV/\mu s$  for different topologies for the inverter.

## 4.4 A more realistic case

For these simulations, the risetime of the PWM pulse was lowered to values that are within the reach of researchers estimates on what SiC-MOSFETS will be able to handle in the near future, which is  $50 \text{ kV}/\mu\text{s}$  [81]. The same estimation, that the switches can be series connected and controlled at the exact same time was done also here as described in Fig. 3.6. The voltages for the generator with different PWMs is shown in Tab. 4.3.

**Table 4.3:** Difference in voltage between 2-, 3- and 5 level PWM for inverters with the same DC-link voltage of  $5 \text{ kV}$ . The simulations are made on a 3 phase system, 100m cable, 72  $\pi$ -sections and the generator rated for  $2.8 \text{ kV}$ .

Number of voltage levels	Maximum line to line voltage [ $\text{kV}$ ]	Maximum neutral to ground voltage [ $\text{kV}$ ]	$dV/dt$ [ $\frac{\text{kV}}{\mu\text{s}}$ ]
2 level	43.26	11.79	50
3 level	23.77	4.51	25
5 level	13.57	4.22	12.5

Table 4.3 shows that there still are unacceptably high voltages at the generator. The line-to-line voltages are lower than for the case with an ideally fast risetime. However, as explained in the theory it will not be significantly lower. What is needed is to implement a filter that can filter out the high frequency components and thereby remove the overvoltage.

### 4.4.1 Filter design and implementation

When implementing filters to the circuit that has been simulated earlier, the behaviour of the system changes. The result of introducing filters is that the high frequency components are significantly affected. The filter that is applied here is an LCR-filter which is connected to the inverter side of the system. By using (2.34) to (2.36) and the system parameters, the filter parameters can be found to be

$$R_{LCR} = 95.3\Omega$$

$$L_{LCR} = 0.292 \text{ mH}$$

$$C_{LCR} = 270 \text{ nF}.$$

When implementing the filter at the inverter side, the risetime of the input voltage to the cable is greatly increased and therefore the  $dv/dt$  of the PWM pulses is decreased. The high frequencies are filtered out and this can be seen in Fig. 4.9 where the  $dv/dt$  of the voltage after the filter is not as sharp as the bottom curve which is the input voltage from the inverter. When the high frequencies are filtered out and the risetime becomes longer, the voltage at the generator terminal decrease greatly compared to without filter. The reduction in voltage on the generator terminal depends on the longer risetime which reduce the reflection at the motor terminal, as was shown in Fig. 4.1 and is also shown in Fig 4.9. It can be noticed from Fig. 4.9 that when the risetime is long enough the reflection is below twice the pulse magnitude, as described by (2.25).

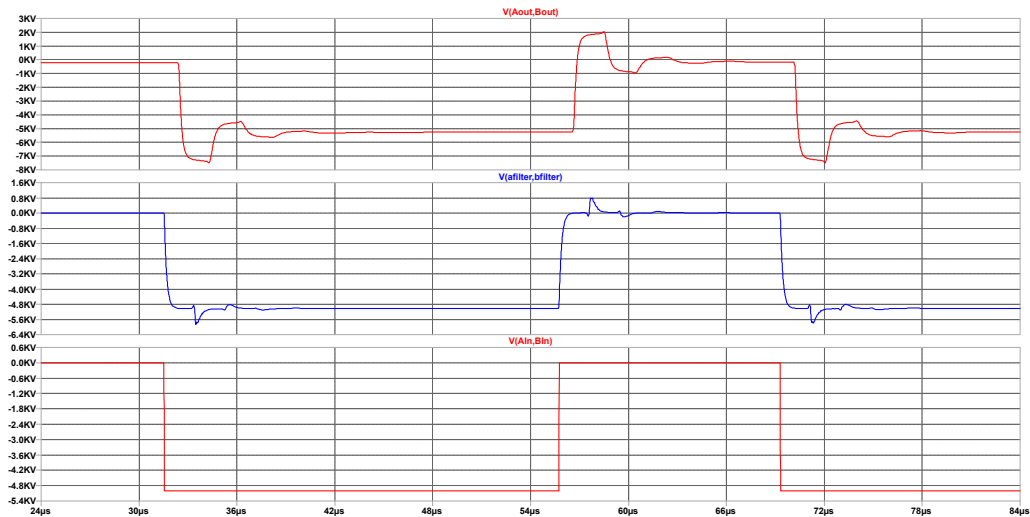


**Figure 4.9:** Waveform of the voltage with filter implemented. The red curve at the bottom is the voltage from the inverter, blue waveform is the voltage after the filter and the top red curve is the generator terminal voltage.

It can be seen from Table 4.4 to 4.6 that with the same LCR filter the  $V_{LL}$  at the generator terminal is the same for different filter topologies. For the three different PWMs the filter topology with a grounded capacitor point has the overall best result when it comes to the common mode voltage. The diode clamped have a better result for 3-level PWM but higher common mode voltage in the other cases.

By looking at Tables 4.4 to 4.6 it can be seen that the line-to-line voltage is reduced with an increase in converter levels, which is expected. It can also be seen that with a 5-level converter the filter is not as needed as it is for 2-level, which suggest that a smaller filter can be used for a 5-level converter than for a 2-level.

The neutral to ground voltage shows the same behaviour with in general, a lower voltage for higher converter levels. However, depending on how the y-connection of the filters is connected the voltage varies quite a lot. This is due to the lack of mutual impedance connection between the phases and the voltage difference created by the PWM pulses. This voltage is described in (2.3), having differences in the common mode voltage depending on the y-connection of the filters is expected since the LCR filter is more effective for the differential mode filter, as (2.2) describes. The common mode voltage can be improved, by using this method, by further increasing the LCR-filter to the point where the signal becomes completely sinusoidal, however that would make the filter unreasonably large.

#### 4. Results

---

**Table 4.4:** Difference in voltage between implementation of different filters, 2-level PWM, 100ns risetime, 2.8kV LL, damping ratio of 1.45.

<b>Filter type</b>	<b>Maximum line to line voltage [kV]</b>	<b>Maximum neutral to ground voltage [kV]</b>
<b>No filter</b>	43.26	11.79
<b>LCR floating</b>	6.19	9.23
<b>LCR grounded</b>	6.19	8.81
<b>LCR diode clamped</b>	6.19	8.60
<b>LCR DC-link clamped</b>	6.19	8.81

**Table 4.5:** Difference in voltage between implementation of different filters, 3-level PWM, 100ns risetime 2.8kV LL, damping ratio of 1.45.

<b>Filter type</b>	<b>Maximum line to line voltage [kV]</b>	<b>Maximum neutral to ground voltage [kV]</b>
<b>No filter</b>	21.52	4.52
<b>LCR floating</b>	5.56	5.77
<b>LCR grounded</b>	5.56	3.91
<b>LCR diode clamped</b>	5.56	4.16
<b>LCR DC-link clamped</b>	5.56	3.92

**Table 4.6:** Difference in voltage between implementation of different filters, 5-level PWM, 100ns risetime 2.8kV LL, damping ratio of 1.45.

<b>Filter type</b>	<b>Maximum line to line voltage [kV]</b>	<b>Maximum neutral to ground voltage [kV]</b>
<b>No filter</b>	13.57	4.22
<b>LCR floating</b>	5.29	4.44
<b>LCR grounded</b>	5.29	4.33
<b>LCR diode clamped</b>	5.29	4.44
<b>LCR DC-link clamped</b>	5.29	4.33

The resulting waveform after the implementation of a 5-level converter and a grounded LCR-filter can be seen in Fig. 4.10. The line-to-line voltage at the generator terminal is after the implementations greatly improved. The voltage does not show any overvoltages due to reflections above the set level to 20% and is thereby regarded as an acceptable voltage according to this project description. The neutral voltage is improved as well.

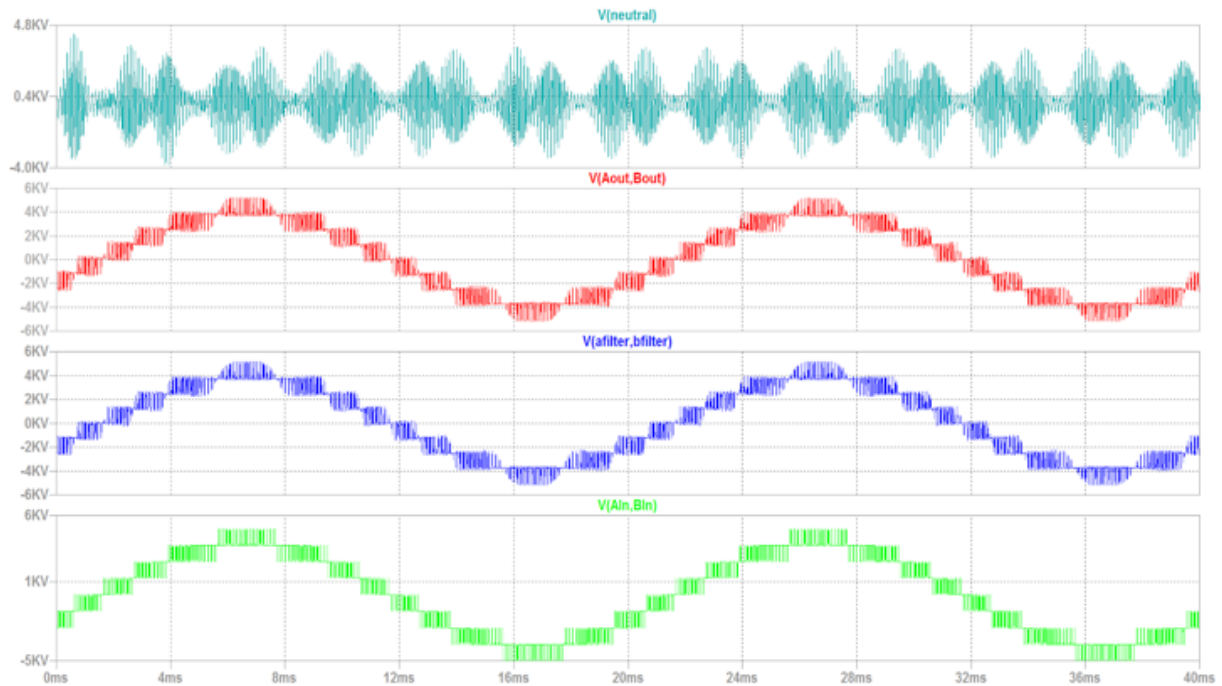
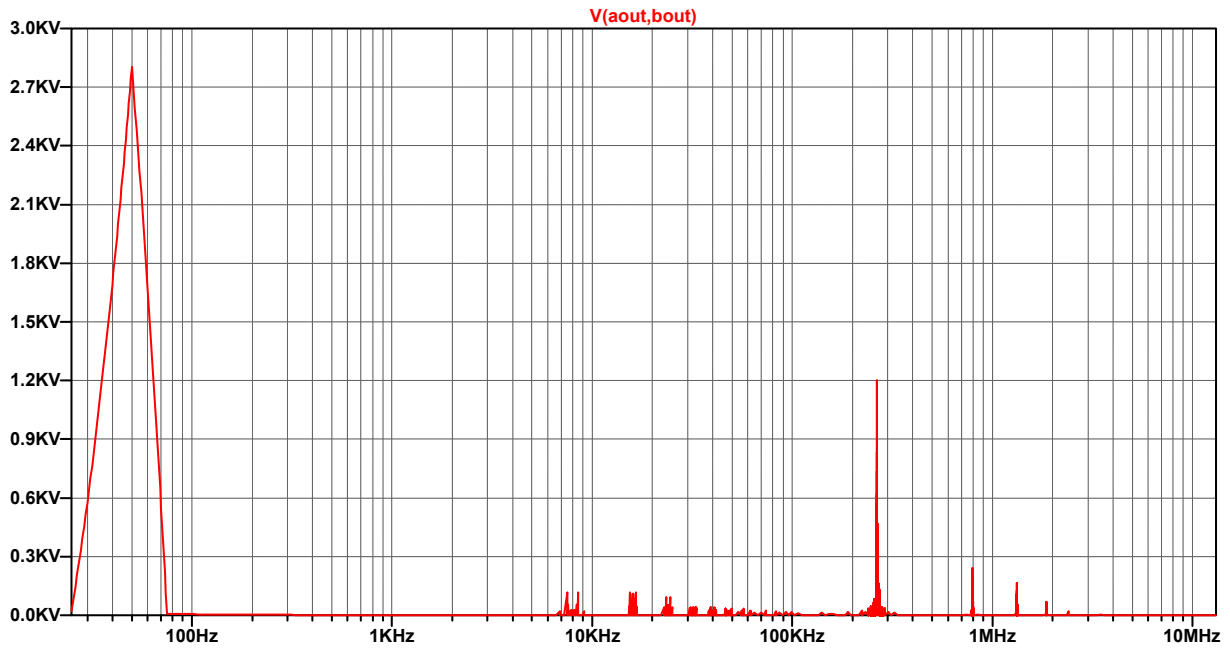


**Figure 4.10:** Waveform of the voltage for the realistic case after 5-level converter and the filter have been implemented

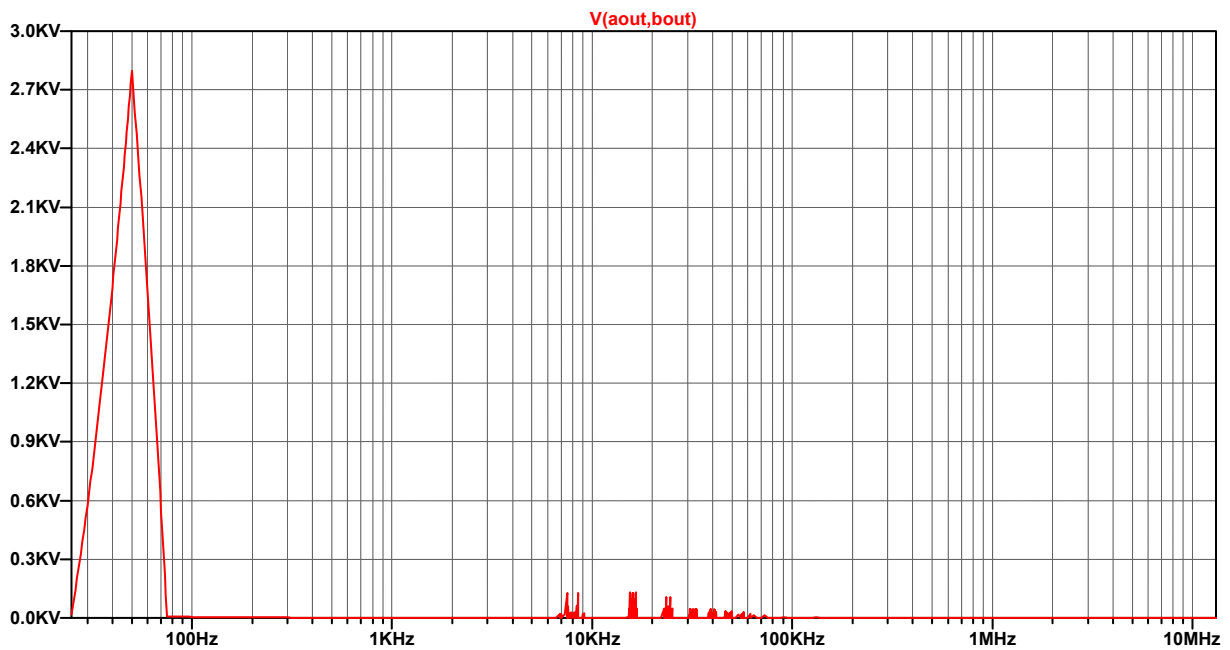
#### 4.4.2 FFT analysis

With the introduction of filters it is clear that the voltage is improved. The overvoltage can be limited to acceptable values by only an LCR filter at the inverter side of the system. As can be seen in the FFTs the reflection frequencies have been eliminated from the system and the switching frequency multiples are reduced. The high frequency content is mitigated by the filter as can be seen in Fig. 4.11, it shows that the reflection frequency is very high when no filter is implemented. When implementing a filter and reducing the  $dV/dt$  the reflection frequency of about 270kHz, as described in the theory, is completely mitigated.

## 4. Results



(a) FFT of the realistic case without filter.



(b) FFT of the line-line voltage of the realistic case with filter implemented.

**Figure 4.11:** The Figure shows 5-level PWM with a  $dv/dt$  of  $12.5kv/\mu s$

### 4.4.3 Reducing filter size

To maintain the voltage limit at the generator terminal at 20% of the DC-link when the voltage levels are increased the capacitance of the filter is changed. A lower value can be chosen since the inverter topology and thereby the  $dV/dt$  of the pulses have changed. However, the two level converter still has a too high neutral voltage. This is shown in table 4.7. Thus, when using an inverter topology with a higher number of levels the neutral voltage is decreased

and the filter size can be reduced.

The LCR-filter parameters can be changed to get a different characteristic from the filter. By changing the capacitance, which the filter design method can through the damping constant from (2.36), the overvoltage can be tuned to a specific voltage. The frequency content can be tuned so that the capacitor removes the high frequency content and thereby lowers the overvoltage.

**Table 4.7:** New values of the capacitor to keep overvoltages at 20% of the DC-link. The inductance and resistance are kept constant. The simulation is for a cable of 100m and 5-level PWM with 100ns risetime and 2.8kV line-line.

Inverter	Capacitance	Voltage line to line [kV]	Damping ratio = $\zeta$	Neutral voltage [kV]
2-level	440nF	6.0	1.85	8.5
3-level	93nF	6.0	0.85	4.2
5-level	32nF	5.9	0.5	4.5

When reducing the inductance of the filter there is a large required change needed for the capacitor in order to keep the voltage within the same levels. By increasing the inductor to a larger one the risetime is reduced and also the overvoltage. This is also shown in table 4.8. With a reduction of the inductance of 20% the capacitance needs to be changed from 440nF to 1F. This shows that the inductance is more important to keep at the designed value for this kind of LCR filter.

**Table 4.8:** The tables shows how the value of the capacitance in the filter need to be adjusted when the inductance is reduced while keeping voltage level below 6kV line-to-line.

Percent of inductance	Capacitance
Inductance 100%	440 nF
Inductance 80%	1 F

With a higher resistance less current will go through the shunt connected part of the filter and thereby less of the high frequencies will be filtered out. There is a shift in the content of the switching harmonics. The results of changing the resistance of the LCR-filter is presented in Table 4.9. It can be seen that by deviating the resistance of the filter from the cable impedance the overvoltage increases. Therefore, the most successful filter have a resistance that match the impedance of the cable in this case 95.3 $\Omega$ .

**Table 4.9:** Reduction of resistance while keeping line-to-line voltage below 6kV

Parameters	Voltage line-to-line [kV]
Resistance 100% (95.3 ohm)	6kV
Resistance 300%	9.4kV
Resistance 10%	9.5 kV



# 5

## Discussion

### 5.1 Findings

From the results it is possible to see that using a higher level PWM switching method will reduce the overvoltages on the generator when being controlled over a long transmission cable. It is quite clear that an implementation of a 5-level inverter has less problems with the voltage compared to a 2-level inverter. By increasing the number of voltage levels in the PWM the differential mode voltage is significantly reduced. From 2-level to 3-level the voltage step is reduced by half and it results in the opportunity of using a smaller filter, which can be extended to 5-level as well. However, it should be noted that these results are exaggerated compared to a real life situation with no experiments to back up the results, and should be recognized as such.

When having an offshore power plant having large components are unwanted. The location of the components make a large impact on the complexity of the overall system. By moving as much of the the power electronic components out of the power plant itself the system becomes easier to physically handle. A reduction in filter size makes installation and maintenance better, which can be achieved by using a 5-level inverter to control the PMSG.

#### 5.1.1 Possible other solutions

Instead of using filters to protect the generator from overvoltages one can instead increase the insulation of the generator so it can withstand higher voltages. When the generator breaks down is dependent on how it is built and how it is insulated. If the filter for some reason cannot be improved it is possible to increase the robustness of the generator. One such way might be to change the way the winding of the generator are wound. If there are two phases in one slot the insulation of those windings will have to withstand the full line to line voltage. By having just one phase per slot that problem is reduced to only the phase voltage. However, by accepting the high overvoltages the power production will most likely be of bad quality.

Another solution to limit the over voltage is to put a line termination network at the generator. The solution presented in this project is a filter at the inverter side. If the situation permits some components in the power plant a terminator filter at the generator side could be implemented.

By reducing the switching frequency of the inverter the phenomenon with voltage interference can be limited. If the voltage magnitude is the main concern it could prove a simple

solution to reducing the overvoltage.

DC transmission always has, for a given voltage and a given cable, lower losses as compared to an AC transmission [45]. DC transmission will be more effective compared to AC transmission with an increase in distance [4]. In the future, this and other types of offshore technology can reduce the losses in the transmission by using DC-transmission. Therefore a study to see the problematics of using DC transmission would be of great interest.

### 5.1.2 Practical use of the results

For the results of this report to be of any use while designing a similar system there are a few aspects that should be taken into consideration. The parameters of the cable and generator will most likely be something else that they are in this report. Therefore one needs to review the filters and make sure that the models of the system still are good enough to be used. The risetimes of the inverter have not been the same as commercial products have on the market, they have been faster. By using an off the shelf IGBT the  $dV/dt$  would be lower and the overvoltage would most likely not present itself to be as large as in this report. The voltage for the 2-level case, Table 4.4 is above the  $\Delta V = 20\%$ , which is set as the acceptable voltage. This could be due to the possibility that the risetime in this study have been above what is commonly used in literature.

Since the voltage has been the only concern in this project the currents or the power have not been taken into consideration. That means that the current rating has of the filters needs to be considered.

## 5.2 Limits of results

One of the difficult parts of the simulations using the methods used in this project is to quantify the reliability of the results. Since the results are obtained from software there will be some differences between the simulated results and an experiment. The assumptions that has been made in the project could affect the simulations to have higher overvoltages than they actually have in a similar experiment.

With the design of the cable being dependent on a variety of different aspects the optimal transmission cable have not been in reach of this project. If an optimal cable would have been used the results may have differed a bit. The parameters that have been used were found in tables of off the shelf cables.

By having separately shielded phases the mutual impedances are not taken into account. This results in a limitation in the capacity for reducing the common mode voltage. Since the commonly used method for reducing the common mode voltage is to use a mutual impedance this method is not viable with the model used in this project.

### 5.2.1 Simulation

The method that has been used in this project, simulating equivalent schematics of the system in question, have its advantages and disadvantages. The model is simple and quite fast to implement but when investigating high frequencies LTspice has its limitations. The simulation time for a circuit of the size needed when using  $\pi$ -sections to model is very large. A simulation with fast risetimes on the PWM signal results in simulation times up to 10 hours with simulation files of about 200GB. Because of this a study with this model of longer cables will prove problematic.

The simulations have been performed as transient analysis simulations. This means that every pulse of the PWM can be seen as one transient but is also the steady state of the system. This is problematic when using LTspice but is the best option available.

### 5.2.2 Sensitivity of component parameters

The phenomenon with reflections and overvoltages are completely dependent on the systems parameter values. Reflections occurs when there is a miss match between the impedances of the components in the system. When changing the values of the parameters of the components in the PTO the overvoltages and reflection changes, this can be seen in a sensitivity analysis. Depending on the design of the generator the values of the parameters can change and therefore alter the results.

## 5.3 Environmental and ethical aspects

When looking at technology that is developed to reduce the carbon footprint of energy production it is interesting to see the impact of parts of that process as well as the whole picture.

### 5.3.1 Environmental

The installation of sub sea equipment will have some environmental effect [7]. The installation itself will damage the sea floor and having the equipment there will also interfere with the aquatic life. However, depending on the state of the sea bottom prior to the installation of the foundation for the power plant it could be beneficial for the aquatic life in the vicinity. The introduction of offshore equipment have been shown to act as artificial reefs that helps the aquatic life. Having the kite move through the water could prove problematic to some sea creatures, small fish might get caught in the turbine and larger marine mammals and large fish could get hit by the moving kite. This too has not, from the testing, proven a problem. No such occurrence has happened.

The use of material is important when choosing which which cable to use when transmitting power. The cables have different impact on the environment depending on which materials that are used. Cables with a long lifetime has less environmental impact since it does not require maintenance or replacement as often.

### 5.3.2 Ethical

In this work some negative aspects of the power production has been of focus. The models used in this project have been exaggerated to see how the problem might look like with inverter technology, that is now in development, were to be used. By exaggerating some negative aspect it can be difficult to comprehend the actual situation as it is today. That is why the assumptions are clearly explained.

Since the high frequency components are not usually included in data sheets from production companies nor a high frequency model it is difficult to find a model that fairly can represent what is happening in this, and in similar systems. To get the model usable for other system configurations the assumptions have been quite rough. Having the phases separately shielded is uncommon and can make a similar case quite different if they are not. However, this simplification have in this case been deemed necessary to keep the variables to a minimum.

# 6

## Conclusion

This project has investigated the problematics of controlling a PMSG system with a PWM inverter connected through long transmission cables. Given the system requirements and depending on the parameters of the generating system there will be a significant difference in the overvoltage that the system can experience. With a simulation and literature study these parameters have been investigated.

The results show that with a 5-level converter with a longer risetime the overvoltage on the generator terminal is greatly reduced compared to a 2-level converter with a faster risetime. The model behaves as the theory describes and is therefore concluded to be sufficient for the study, with its assumptions. In addition, by introducing filters to the system the overvoltage on  $V_{LL}$  is reduced to an acceptable voltage.

It was found that the inverter topology, switching method and switching time greatly affects how the generator terminals react to the voltage pulses. By changing the inverter topology and risetime, the overvoltage at the generator changes and different filters are needed. If the aim is to reduce the size of the submerge part of the system, one can apply the changes to the system that are proposed in this report. These changes are: use a multilevel converter; match the impedance of the generator with the impedance of the cable by designing the geometry; use a terminator at the generator terminal to reduce the reflection coefficient as much as possible.

### 6.1 Future work

In the future, when this work is continued to be worked on the authors of this project suggest that an even more accurate model should be developed by measuring on a generator that is, if not the one, a similar one to the one to be used in the complete system. By measuring with an RLC meter and finding the parameter values and how they vary with frequency and perhaps heat and current the model would be greatly improved. That way the results would be easier to quantify and that would lead to a stronger conclusion.

Another thing that should be done in the future is to verify the results and compare to a real case. In this project there was no opportunity to confirm the studies performed. This project should be completed with data from a case with real components and a functioning system.

During the effective on-time of the tidal power plant the possible power output is not always at rated power. With the difference in tidal current the output will change. For future work

## 6. Conclusion

---

this aspect should preferably be investigated. For the times when the tidal current flow is not high enough to give the power plant the resource to produce rated power there are fluctuations in the power produced as well. This scenario could possibly produce disturbances in the voltage and power that could produce difficulties in the rest of the power take off system.

# Bibliography

- [1] E. Singhroy, "Taming Dragons, Improving power performance of tethered turbine tidal farms," 2017.
- [2] R. H. Charlier and C. W. Finkl, *Ocean Energy*, 2009.
- [3] C. Purcarea, *PhD Dissertation*.
- [4] M. Kuschke and K. Strunz, "Transient cable overvoltage calculation and filter design: Application to onshore converter station for hydrokinetic energy harvesting," *IEEE Transactions on Power Delivery*, vol. 28, no. 3, pp. 1322–1329, 2013.
- [5] Z. M. Mcalister, Dzurko, H. A. Walker, and Group, "Machine design and control strategy for wide-speed-range PMSG systems," 1991.
- [6] E. Persson, "Transient Effects in Application of PWM Inverters to Induction Motors," *IEEE Transactions on Industry Applications*, vol. 28, no. 5, pp. 1095–1101, 1992.
- [7] T. Worzyk, *Submarine Power Cables*, 2009, vol. 53, no. 9. [Online]. Available: <http://link.springer.com/10.1007/978-3-642-01270-9>
- [8] L. A. Saunders, G. L. Skibinski, M. La, S. T. Evon, K. Mountain, and D. L. Kempkes, "Riding the Reflected Wave IGBT Drive Technology," *October*, 1996.
- [9] T. L. Van, T. D. Nguyen, T. T. Tran, and H. D. Nguyen, "Advanced control strategy of back-to-back PWM converters in pmsg wind power system," *Advances in Electrical and Electronic Engineering*, vol. 13, no. 2, pp. 81–95, 2015.
- [10] J. Tang, S. Lundberg, F. Marra, and Y. Liu, "Sensorless control of a PMSM with a transmission system including shunt branches," *Proceedings - 2016 22nd International Conference on Electrical Machines, ICEM 2016*, pp. 1160–1166, 2016.
- [11] M. C. Sousounis, J. K. H. Shek, and M. A. Mueller, "Filter design for cable overvoltage and power loss minimization in a tidal energy system with onshore converters," *IEEE Transactions on Sustainable Energy*, vol. 7, no. 1, pp. 400–408, 2016.
- [12] A. Von Jouanne and P. N. Enjeti, "Design considerations for an inverter output filter to mitigate the effects of long motor leads in ASD applications," *IEEE Transactions on Industry Applications*, vol. 33, no. 5, pp. 1138–1145, 1997.
- [13] N. Hanigovszki, J. Landkildehus, G. Spiazzi, and F. Blaabjerg, "An EMC evaluation of the use of unshielded motor cables in AC adjustable speed drive applications," *IEEE Transactions on Power Electronics*, vol. 21, no. 1, pp. 273–280, 2006.
- [14] K. Gulez and A. A. Adam, "High-frequency common-mode modeling of permanent magnet synchronous motors," *IEEE Transactions on Electromagnetic Compatibility*, vol. 50, no. 2, pp. 423–426, 2008.
- [15] P. T. Ioannis, "Modulation techniques low voltage drives and their system aspects," presented at ICEM, XXIIIrd International Conference on Electrical Machines (ICEM'2018), Ramada Plaza Thraki Alexandroupoli - Greece, 2018.

- [16] D. Xu, Q. Gao, and W. Wang, "Design of a passive filter to reduce common-mode and differential-mode voltage generated by voltage-source PWM inverter," *IECON Proceedings (Industrial Electronics Conference)*, pp. 2483–2487, 2006.
- [17] C. Cooper, *IEEE Recommended Practice for Electric Power Distribution for Industrial Plants*, 1988, vol. 2, no. 2. [Online]. Available: <http://digital-library.theiet.org/content/journals/10.1049/pe{ }19880018>
- [18] V. Sarac and D. Iliev, "Synchronous Motor of Permanent Magnet compared to Asynchronous Induction Motor," 2000.
- [19] M. Zoghlami, R. Kharoui, N. Fnaeich, and F. Bacha, "Direct Power Control Strategy for Variable Speed Wind Energy Conversion System Based on PMSM Generator," pp. 1348–1353, 2016.
- [20] R. Krishnan, "Application Characteristics of Permanent Magnet Synchronous and Brushless dc Motors for Servo Drives," *IEEE Transactions on Industry Applications*, vol. 27, no. 5, pp. 986–996, 1991.
- [21] S. Chapman, *Electric machinery fundamentals*, 2012.
- [22] F. Kendouli, K. Abed, K. Nabti, H. Benalla, and B. Azoui, "High performance PWM converter control based PMSG for variable speed wind turbine," *2012 First International Conference on Renewable Energies and Vehicular Technology*.
- [23] M. Melfi, A. M. Jason Sung, S. Bell, and G. L. Skibinski, "Effect of surge voltage risetime on the insulation of low-voltage machines fed by pwm converters," *IEEE Transactions on Industry Applications*, vol. 34, no. 4, pp. 766–775, 1998.
- [24] O. Carlson, "Sustainable Power Production and Transportation," 2017.
- [25] A. Hughes and B. Drury, *Synchronous and Brushless Permanent Magnet Machines and Drives*, 2013. [Online]. Available: <http://linkinghub.elsevier.com/retrieve/pii/B9780080983325000097>
- [26] A. H. Kasem Alaboudy, A. A. Daoud, S. S. Desouky, and A. A. Salem, "Converter controls and flicker study of PMSG-based grid connected wind turbines," *Ain Shams Engineering Journal*, vol. 4, no. 1, pp. 75–91, 2013. [Online]. Available: <http://dx.doi.org/10.1016/j.asej.2012.06.002>
- [27] Masoum, M. A.S., Fuchs, and E. F., "*Power Quality in Power Systems and Electrical Machines (2nd Edition)*", 2015.
- [28] B. S. Oyegoke, "Comparative analysis of methods for calculating the transient voltage distribution within the stator winding of an electric machine subjected to steep-fronted surge," *Electrical Engineering*, vol. 82, no. 3, pp. 173–182, 2000.
- [29] S. Bell and J. Sung, "Will your motor insulation survive a new adjustable-frequency drive?" *IEEE Transactions on Industry Applications*, vol. 33, no. 5, pp. 1307–1311, 1997.
- [30] M. Fenger and G. Stone, "Progress in understanding the nature of PF in stators created by inverter drives," pp. 363–368, 2003.
- [31] J. M. Martínez, H. Amarís, and J. Sanz, "Frequency domain modelling of random wound motor windings for insulation stress analysis," *Electrical Engineering*, vol. 88, no. 5, pp. 403–409, 2006.
- [32] T. Cedex and M. L. Somer, "Rotating machines supplied by inverters." pp. 792–795, 1994.
- [33] J. A. Oliver and G. C. Stone, "Implications for the Application of Adjustable Speed Drive Electronics to Motor Stator Winding Insulation," *IEEE Electrical Insulation Magazine*, vol. 11, no. 4, pp. 32–36, 1995.

- [34] G. Skibinski, J. Erdman, J. Pankau, and J. Campbell, "Assessing AC motor dielectric withstand capability to reflected voltage stress using corona testing," *IAS '96. Conference Record of the 1996 IEEE Industry Applications Conference Thirty-First IAS Annual Meeting*, vol. 1, pp. 694–702, 1996. [Online]. Available: <http://ieeexplore.ieee.org/lpdocs/epic03/wrapper.htm?arnumber=557114>
- [35] B. Soediono, "Electrical Insulation for Rotating Machines," *Journal of Chemical Information and Modeling*, vol. 53, p. 160, 1989.
- [36] J. Belhadj and X. Roboam, "Investigation of Different Methods to Control a Small Variable-Speed Wind Turbine With PMSM Drives," *Journal of Energy Resources Technology*, vol. 129, no. 3, p. 200, 2007. [Online]. Available: <http://energyresources.asmedigitalcollection.asme.org/article.aspx?articleid=1414707>
- [37] A. Videt, P. Le Moigne, N. Idir, P. Baudesson, J. J. Franchaud, and J. Ecrabey, "Motor overvoltage limitation by means of a new EMI-reducing PWM strategy for three-level inverters," *IEEE Transactions on Industry Applications*, vol. 45, no. 5, pp. 1678–1687, 2009.
- [38] N. Mohan, *Power electronics, converters applications and design*, 2003.
- [39] T. G. Arora and M. M. Renge, "Effects of Switching Frequency and Motor Speed on Common Mode Voltage, Common Mode Current and Shaft Voltage in PWM Inverter-fed Induction Motors," pp. 583–588, 2017.
- [40] R. J. Kerkman, D. Leggate, D. Schlegel, and G. Skibinski, "PWM inverters and their influence on motor over-voltage," *Applied Power Electronics Conference and Exposition*, vol. 53092, no. 414, pp. 103–113, 1997.
- [41] V. Naumanen, J. Korhonen, P. Silventoinen, and J. Pyrhonen, "Mitigation of high du/dt-originated motor overvoltages in multilevel inverter drives," *IET Power Electronics*, vol. 3, no. 5, p. 681, 2010. [Online]. Available: <http://digital-library.theiet.org/content/journals/10.1049/iet-pel.2009.0171>
- [42] P. C. Systems, *IEEE Guide for the Planning, Design, Installation, and Repair of Submarine Power Cable Systems*, 2005, no. March.
- [43] R. T. Traut, "Underwater power cables."
- [44] IEEE, *IEEE Standard 835 - IEEE Standard Power Cable Ampacity Tables*, 2012, vol. 1994 (R201).
- [45] F. Wang, Y. Pei, D. Boroyevich, R. Burgos, and K. Ngo, "Ac vs. dc distribution for off-shore power delivery," *IECON Proceedings (Industrial Electronics Conference)*, pp. 2113–2118, 2008.
- [46] H. Saadat, *Power System Analysis*, 2010.
- [47] N. Idir, Y. Weens, and J. J. Franchaud, "Skin effect and dielectric loss models of power cables," *IEEE Transactions on Dielectrics and Electrical Insulation*, vol. 16, no. 1, pp. 147–154, 2009.
- [48] G. J. Anders, *Rating of electric power cables in unfavorable thermal environment*, 2004.
- [49] J. Dickinson and P. J. Nicholson, "Calculating the high frequency transmission line parameters of power cables," *Isplc*, 1997.
- [50] R. Bartnikas, *Power and Communication cables: Theory and applications*, 2000.
- [51] Mathworks. PI Section Line, Accessed: 2018-08-31. [Online]. Available: <https://se.mathworks.com/help/physmod/sps/powersys/ref/pisectionline.html>

- [52] P. Enjeti, A. Von Jouanne, and W. Gray West, "The effect of long motor leads on PWM inverter fed AC motor drive systems," *Electrical Engineering*, vol. 2, no. 1, pp. 592–597, 1995.
- [53] P. G. Stations, "IEEE Guide for the Design and Installation of Cable Systems in Power Generating Stations," vol. 1986, 1986.
- [54] Y. Weens, N. Idir, R. Bausière, and J. J. Franchaud, "Modeling and simulation of unshielded and shielded energy cables in frequency and time domains," *IEEE Transactions on Magnetics*, vol. 42, no. 7, pp. 1876–1882, 2006.
- [55] J. Blennow, "Lecture notes, Wave impedance and traveling waves, High voltage engineering," 2016.
- [56] L. V. Bewley, "Traveling Waves on Transmission Systems," *Transactions of the American Institute of Electrical Engineers*, vol. 50, no. 2, pp. 532–550, 1931. [Online]. Available: <http://ieeexplore.ieee.org/document/5055827/>
- [57] R. J. Kerkman, D. Leggate, and G. L. Skibinski, "Interaction of drive modulation and cable parameters on ac motor transients," *IEEE Transactions on Industry Applications*, vol. 33, no. 3, pp. 722–731, 1997.
- [58] S. Lee and K. Nam, "An overvoltage suppression scheme for ac motor drives using a half dc-link voltage level at each PWM transition," *IEEE Transactions on Industrial Electronics*, vol. 49, no. 3, pp. 549–557, 2002.
- [59] C. J. Melhom and L. Tang, "Transient Effects of PWM ASDs on Standard Squirrel Cage Induction Motors," pp. 2689–2695, 1995.
- [60] G. Skibinski, D. Leggate, and R. Kerkman, "Cable characteristics and their influence on motor over-voltages," *Proceedings of APEC 97 - Applied Power Electronics Conference*, vol. 1, pp. 114–121. [Online]. Available: <http://ieeexplore.ieee.org/document/581441/>
- [61] S. Lee, "Overvoltage Suppression Filter Design Methods Based on," *Design*, vol. 19, no. 82, pp. 1808–1812, 2003.
- [62] G. Skibinski, R. Kerkman, D. Leggate, J. Pankau, and D. Schlegel, "Reflected wave modeling techniques for PWM AC motor drives," *APEC '98 Thirteenth Annual Applied Power Electronics Conference and Exposition*, vol. 2, no. c, pp. 1021–1029, 1998.
- [63] A. Von Jouanne, D. A. Rendusara, P. N. Enjeti, and J. W. Gray, "Filtering techniques to minimize the effect of long motor leads on pwm inverter-fed ac motor drive systems," *IEEE Transactions on Industry Applications*, 1996.
- [64] J. K. Shek, M. C. Sousounis, and M. A. Mueller, "Modelling, control and frequency domain analysis of a tidal current conversion system with onshore converters," *IET Renewable Power Generation*, vol. 10, no. 2, pp. 158–165, 2016. [Online]. Available: <http://digital-library.theiet.org/content/journals/10.1049/iet-rpg.2014.0331>
- [65] M. C. Sousounis, "Electro-Mechanical Modelling of Tidal Arrays," 2018.
- [66] C. Jettanassen, "Passive common-mode EMI filter adapted to an adjustable-speed AC motor drive," *2010 9th International Power and Energy Conference, IPEC 2010*, no. 1, pp. 1025–1030, 2010.
- [67] Merhej Saad J. and Nichols William H., "Harmonic Filtering for the Offshore Industry," *IEEE Transactions on Industry Applications*, vol. 30, no. 3, pp. 533–542, 1994.
- [68] F. J. T. Arthur B. Williams, *Electronic Filter Design Handbook, Fourth Edition*, 2006.
- [69] E. F. Fuchs, *The Roles of Filters in Power Systems*, 2008. [Online]. Available: <http://linkinghub.elsevier.com/retrieve/pii/B9780123695369500103>

- [70] G. Skibinski, "Design methodology of a cable terminator to reduce reflected voltage on AC motors," *Industry Applications Conference, 1996. Thirty-First IAS Annual Meeting, IAS '96., Conference Record of the 1996 IEEE*, vol. 1, pp. 153–161 vol.1, 1996.
- [71] J. He, G. Y. Sizov, P. Zhang, and N. A. Demerdash, "A review of mitigation methods for overvoltage in long-cable-fed PWM AC drives," *IEEE Energy Conversion Congress and Exposition: Energy Conversion Innovation for a Clean Energy Future, ECCE 2011, Proceedings*, no. 1028348, pp. 2160–2166, 2011.
- [72] N. Hanigovski, J. Poulsen, and F. Blaabjerg, "A novel output filter topology to reduce motor overvoltage," *IEEE Transactions on Industry Applications*, vol. 40, no. 3, pp. 845–852, 2004.
- [73] J. C. Das, "Passive Filters - Potentialities and Limitations," *IEEE Transactions on Industry Applications*, vol. 40, no. 1, pp. 232–241, 2004.
- [74] B. Abb, "Power Cable Systems."
- [75] J. Tang, "Control of a subsea PMSM with a very long feeding cable using a top-side converter – design and performance evaluation Master of Science Thesis Junfei Tang," p. 183, 2016.
- [76] T. Ohno and A. Ametani, "Cable Modeling for Transient Simulations," *Cable System Transients: Theory, Modeling and Simulation*, pp. 163–184, 2015.
- [77] A. F. Moreira, T. A. Lipo, G. Venkataramanan, and S. Bernet, "High-frequency modeling for cable and induction motor overvoltage studies in long cable drives," *IEEE Transactions on Industry Applications*, vol. 38, no. 5, pp. 1297–1306, 2002.
- [78] G. Grandi, D. Casadei, and A. Massarini, "High Frequency Lumped Parameter Model for AC Motor Windings," *Journal of Chemical Information and Modeling*, vol. 53, no. 9, pp. 1689–1699, 2013.
- [79] G. Grandi, D. Casadei, and U. Reggiani, "Equivalent circuit of mush wound AC windings for high frequency analysis," *Industrial Electronics, 1997. ISIE '97., Proceedings of the IEEE International Symposium on*, vol. 1, pp. SS201–SS206 vol.1, 1997.
- [80] Infineon. Infineon, IGBT power module datasheet, SKiiP 26ACM12V17, Accessed: 2018-09-19. [Online]. Available: [https://www.infineon.com/cms/en/product/power/igbt/igbt-modules/igbt-modules-up-to-1600v-1700v/fs50r17ke3\\_b17/](https://www.infineon.com/cms/en/product/power/igbt/igbt-modules/igbt-modules-up-to-1600v-1700v/fs50r17ke3_b17/)
- [81] H. Chen and D. Divan, "High speed switching issues of high power rated silicon-carbide devices and the mitigation methods," *2015 IEEE Energy Conversion Congress and Exposition, ECCE 2015*, pp. 2254–2260, 2015.
- [82] G. Kraus and E. Tettang, "SPICE-Simulation using LTspice IV," *System*, pp. 1–76, 2010.